

Fault kinematics: A record of tectono-climatically controlled sedimentation along passive margins, an example from the U.S. Gulf of Mexico

Abah P. Omale^{1,†}, Juan M. Lorenzo¹, Ali AlDhamen², Peter D. Clift¹, and A. Alexander G. Webb³

¹Department of Geology and Geophysics, Louisiana State University, Baton Rouge, Louisiana 70803, USA

²Baker Hughes, Abqaiq Highway, Opp Second Ind City 2, Dhahran, Ash Sharqiyah, Saudi Arabia

³Division of Earth and Planetary Science and Laboratory for Space Research, The University of Hong Kong, Pokfulam Road, Hong Kong

ABSTRACT

Faults offsetting sedimentary strata can record changes in sedimentation driven by tectonic and climatic forcing. Fault kinematic analysis is effective at evaluating changes in sediment volumes at salt/shale-bearing passive margins where sediment loading drives faulting. We explored these processes along the northern Gulf of Mexico. Incremental throw along 146 buried faults studied across onshore Louisiana revealed continual Cenozoic fault reactivation punctuated by inactive periods along a few faults. Fault scarp heights measured from light detection and ranging (LiDAR) data were interpreted to show that Cenozoic fault reactivation continued through the Pleistocene.

The areas of highest fault throw and maximum sediment deposition shifted from southwest Louisiana in the early Miocene to southeast Louisiana in the middle-late Miocene. These changes in the locus of maximum fault reactivation and sediment deposition were controlled by changing tectonics and climate in the source areas. Early Miocene fault throw estimates indicate a depocenter farther east than previously mapped and support the idea that early Miocene Appalachian Mountain uplift and erosion routed sediment to southeast Louisiana.

By correlating changes in fault throw with changes in sediment deposition, we suggest that (1) fault kinematic analysis can be used to evaluate missing sediment volumes because fault offsets can be preserved despite partial erosion, (2) fault throw estimates can be used to infer changes in past tectonic and climate-related processes driving sedimentation, and (3) these observations are applicable to other

passive margins with mobile substrates and faulted strata within overfilled sedimentary basins.


INTRODUCTION

Tectonics and climate are two fundamentally different processes that exert control on the rate of sediment supply to passive margins. Consequently, passive margin stratigraphy can contain a record of the past tectonically driven uplift and climatic changes that affected sediment source areas far from the final depocenter. Current methods for interpreting hinterland exhumation rates and past cold or warm periods from the sedimentary record at passive margins include sequence stratigraphy (Galloway, 1989; Posamentier, 1988; Posamentier et al., 1988; Vail et al., 1977; Van Wagoner et al., 1988), chemostratigraphy (Mountain et al., 2007; Weissert et al., 2008), sediment provenance analysis (Cawood et al., 2003; Fedo et al., 2003; Galloway et al., 2011; Haughton et al., 1991), and geochronology (Busby et al., 1995, 2012; Gehrels, 2011; Xu et al., 2017; Fig. 1 herein). These methods become more difficult to use as erosion in the basin becomes more extensive. However, in extensional settings with overfilled sedimentary basins, the normal fault displacement history affecting any one sedimentary unit is preserved until erosion starts to remove the unit from the footwall. In such cases, it is possible to infer changes in sediment supply from fault kinematics despite partial erosion, whereas any amount of erosion from the footwall of a sedimentary unit reduces the estimated fault offset and leads to underestimated initial sediment thickness.

Passive margins with a mobile substrate and large volume of sediments often display good correlation between fault displacement and sediment supply. Fault displacement within the sediments in the postrift period is caused by sediment loads mobilizing a substrate (e.g., shale or salt)

via differential loading and/or gravity gliding (Brun and Fort, 2011; Hudec and Jackson, 2007; Rowan, 2019; Rowan et al., 2012; Vendeville and Jackson, 1992a, 1992b). Fault slip appears to respond to extra sediment load over short periods of time, when suitable mobile substrates are displaced. During differential loading or gravity gliding, either salt or shale may be withdrawn from beneath major depositional centers or from updip areas of the passive margin and then transported away from the depositional center and/or in a downdip direction. Consequently, mobilization of the underlying mobile substrate leads to extension and normal faulting within the depocenter, as well as contraction and diapiric flow away from the depocenter (Vendeville and Jackson, 1992a, 1992b; Wu et al., 1990). High rates of sediment supply lead to the formation of growth faults as sediment thickness commonly surpasses the fault offset and make these margins the most likely to preserve their faulting history. These processes have been well documented, for example, in the Niger Delta basin, offshore Nigeria, since the Miocene (Doust, 1990; Whiteman, 1982) and in the Santos Basin, offshore Brazil, since the Cretaceous (Demercian et al., 1993; Ojeda, 1982).

The Gulf of Mexico passive margin is a good candidate for the study of these processes because it contains numerous faults initiated and reactivated by large and changing volumes of prograding siliciclastic sediments displacing (highly mobile) salt during the Cenozoic (Diegel et al., 1995; Galloway, 1989; Lopez, 1990; McBride, 1998; Omale and Lorenzo, 2015; Peel et al., 1995; Rowan et al., 1999; Thorsen, 1963; Woodbury et al., 1973; Worrall and Snelson, 1989). The rate of sediment supply during the Cenozoic has been controlled largely by tectonic and climatic changes within the sediment source area, assuming limited, short-term (<10⁶ yr) buffering between the source and the continental margin (Bentley et al., 2016; Blum and Pecha, 2014; Galloway et al., 2011; Winker,

Abah Omale  <http://orcid.org/0000-0002-6858-8301>

[†]aomale1@lsu.edu.

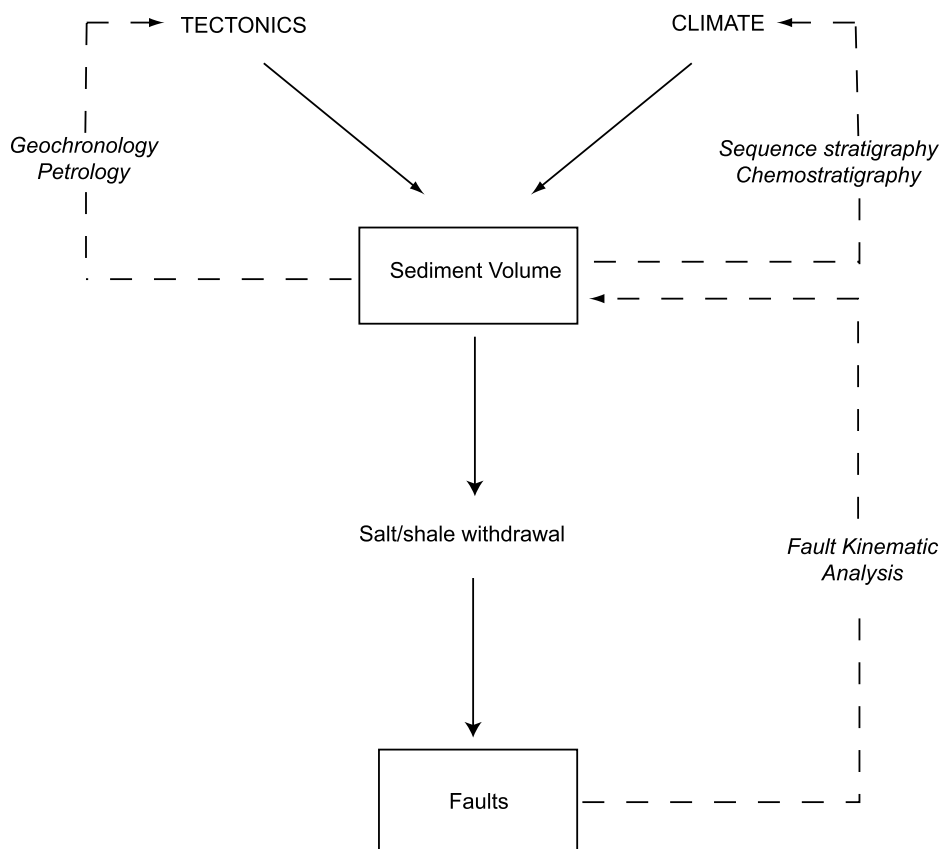


Figure 1. Distal-primary (in uppercase letters) and local-secondary processes (salt/shale withdrawal) and their products (within boxes) at passive margins with mobile substrates. Different techniques (italicized letters) extract the process from the products (within boxes). Note that although sediment volume is a product of tectonic and climatic forcing, it also acts as a control on fault movement by secondary mechanisms (salt/shale withdrawal). Flexure during sediment loading is not considered.

1982). Peak periods of sediment supply during the Cenozoic correlate with peak periods of uplift and denudation in sediment source areas within the western and eastern interior of the North American continent (Bentley et al., 2016; Fernandes et al., 2019; Gallen et al., 2013; Galloway et al., 2011; Liu, 2014, 2015; Xu et al., 2017). At least three periods of major sediment flux (65 Ma, 40–15 Ma; and 5–0 Ma; Galloway et al., 2011) broadly correlate with phases of uplift and magmatism in the Rocky Mountain–Colorado Plateau region, which is the western continental sediment source area for the Gulf of Mexico (Fernandes et al., 2019). The ~1–2 km uplift of the Colorado Plateau and associated magmatism (Roy et al., 2009) since the Cretaceous are attributed to the presence of anomalously warm asthenosphere (Fitton et al., 1991; Roy et al., 2009) beneath a thin lithosphere (Klöcking et al., 2018), as inferred from magma chemistry (Fitton et al., 1991; Roy et al., 2009) and analyses combining shear wave velocities, asthenosphere temperature, and basaltic geo-

chemistry (Klöcking et al., 2018). An increase in sediment supply into the Gulf of Mexico from the eastern continental source area since the Miocene is attributed to the uplift of the Appalachian Mountains related to dynamic topography (Fernandes et al., 2019; Gallen et al., 2013; Liu, 2014, 2015; Miller et al., 2013) and/or accelerated erosion caused by increasing storm intensity (Boettcher and Milliken, 1994; Galloway et al., 2011). The dynamic topography as a cause of Appalachian Mountain uplift may have been an isostatic response to mantle delamination (Gallen et al., 2013), or convective flow within the mantle induced by the downgoing Farallon slab (Liu, 2014, 2015; Miller et al., 2013). In the north-central Gulf Coast (south Louisiana), the early Miocene depocenter is located in southwest and south-central Louisiana, fed by the ancestral Red and Mississippi Rivers, respectively, whereas the middle Miocene depocenters shifted eastward to south-central and southeast Louisiana and were fed by the Mississippi River and paleo-Tennessee River fluvial axes, respec-

tively (Fig. 2; Galloway et al., 2011; Xu et al., 2017). Furthermore, the northern Gulf of Mexico is characterized by onshore fault scarps that reflect the fault displacement history and record the continental-scale sediment supply during the Pleistocene–Holocene interval. Fault displacement resulted from large volumes of prograding Pleistocene and Holocene sediments being supplied and deposited in response to changes in erosion rates during glacial and interglacial cycles (Dokka et al., 2006; Ivins et al., 2007; Shen et al., 2017). The heights and slopes of fault scarps may be used to determine the magnitude and relative ages of fault reactivation episodes (Bucknam and Anderson, 1979; Enzel et al., 1994; Rao et al., 2017; Wallace, 1977). In addition, oil and gas exploration starting in the twentieth century has provided large amounts of regional seismic and well-log data from which fault motion history can be constrained.

In this contribution, we performed kinematic analysis of faults from south Louisiana using light detection and ranging (LiDAR), well-log, and seismic reflection data. We show that major fault offsets indicate periods of maximum sedimentation coeval with tectonic and climatic events within the North American continental interior during the Cenozoic. In addition, by correlating changes in fault throw with changes in sediment supply, we suggest that fault offsets can be used to evaluate missing sediment volumes because fault offsets can be preserved despite partial erosion.

TECTONO-SEDIMENTARY EVOLUTION OF THE NORTHERN GULF OF MEXICO

Geologic Setting

The Gulf of Mexico is an ocean basin that initiated during the Mesozoic breakup of Pangea, following the separation of North America from South America, and developed by crustal extension and seafloor spreading (Buffler et al., 1994; Salvador, 1987). Extension and thermal subsidence have created ~5–7 km of subsidence and accommodation for sediment deposition (Sawyer et al., 1991). Following the incursion of seawater, salt deposition began in the restricted basin prior to and during early seafloor spreading, and it resulted in a thick Jurassic accumulation of autochthonous Louann Salt (~3–4 km thick; Salvador, 1987).

The postsalt depositional history of the Gulf of Mexico basin involved rimmed carbonate platform emplacement and continued subsidence. By the end of the Early Cretaceous, these formed the framework for the present-day basin outline and morphology (Galloway, 2008;

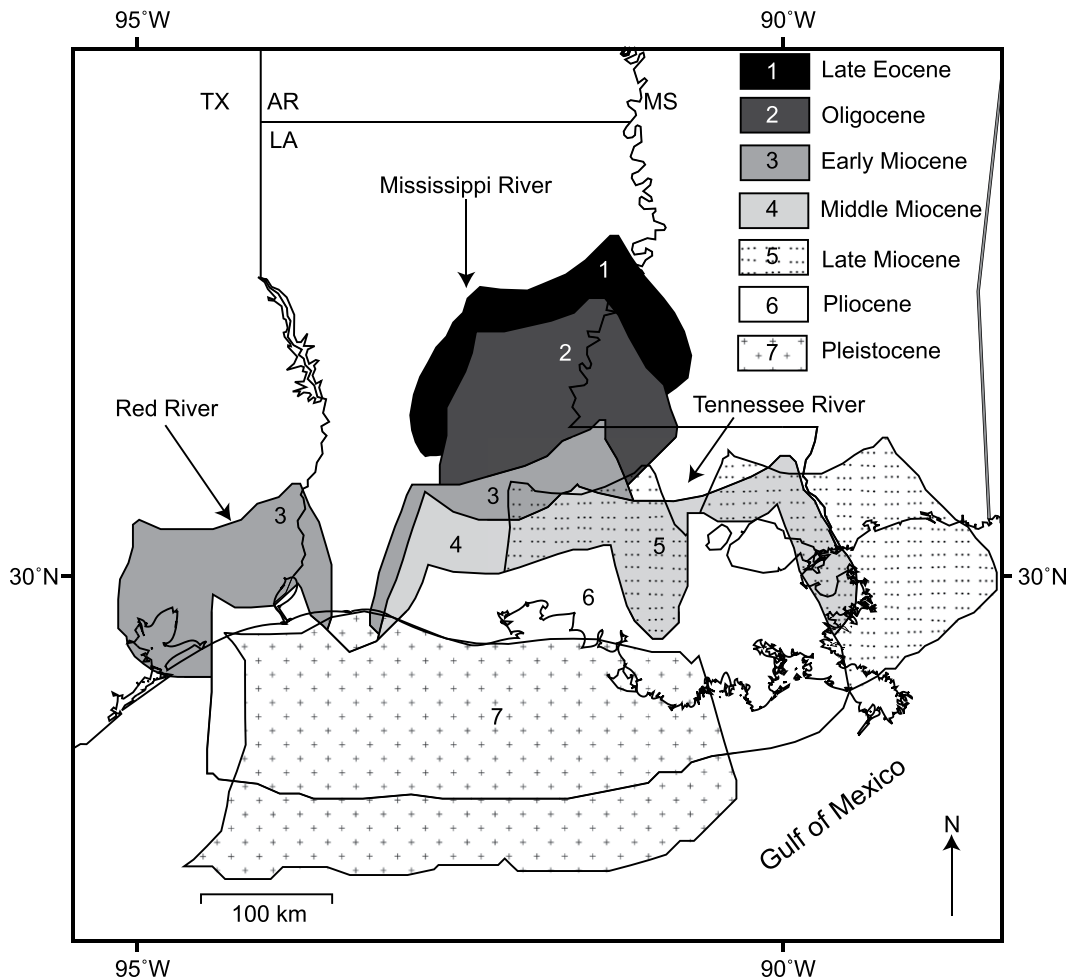


Figure 2. Location of seven sediment depositional centers across northern Gulf of Mexico during the Cenozoic (Galloway et al., 2011). Between late Eocene (1) and middle Miocene (4), centers move generally from north to south. Between early Miocene (3) and late Miocene (5), centers move from southwest to southeast Louisiana. In the Pleistocene (7), the depocenter shifts back toward the west. State abbreviations: AR—Arkansas, LA—Louisiana, MS—Mississippi, TX—Texas. Map projection is World Geodetic System 1984, World Mercator.

Winker and Buffler, 1988). In the Cenozoic, siliciclastic sediment supply and margin progradation became dominant, controlled by tectonic and climatic processes in the hinterland (Bentley et al., 2016; Galloway, 2008; Galloway et al., 2000, 2011) and slowing rates of thermal postrift subsidence. Rapid sediment supply created thick successions and initiated gravity tectonics defined by dominant basinward salt evacuation and consequent fault activity, including growth faulting (Diegel et al., 1995; McBride, 1998; Peel et al., 1995; Rowan, 1995; Schuster, 1996; Winker, 1982; Worrall and Snelson, 1989). Sediment deposition and salt withdrawal created additional accommodation and caused load-induced basin subsidence (e.g., present-day basement depth of ~16–20 km in the northern Gulf of Mexico; Peel et al., 1995). The location, magnitude, and timing of fault activity changed in response to shifts in the location(s) of the dominant sediment supply caused by changes in tectonic and climatic events within the interior of North America (Dokka et al., 2006; Hanor, 1982; Heinrich, 2000; Omale and Lorenzo, 2015; Thorsen, 1963).

In the north-central Gulf of Mexico (south Louisiana), Paleocene–early Eocene clastic progradation driven by faster erosion following Laramide uplift in the central and southern Rocky Mountains led to salt evacuation and growth faulting (Eaton, 2008; Galloway, 2008; Galloway et al., 2005, 2011; McMillan et al., 2002, 2006; Winker, 1982). During the late Eocene–early Miocene, regional crustal heating, uplift, and volcanism in the southwest United States increased erosion and sediment supply mainly to southwest Louisiana (Galloway, 2008; Galloway et al., 2011), resulting in more faulting in that area (Diegel et al., 1995; Omale and Lorenzo, 2015; Peel et al., 1995). Furthermore, large increases in sedimentation rate and fault activity in the Miocene reflect the erosional rejuvenation of the eastern North American (Appalachian) uplands due to regional climate change (Boettcher and Milliken, 1994) and dynamic surface topography (Liu, 2014, 2015), resulting in supply of sediment to large depocenters (Galloway et al., 2011) and strong growth faulting in southeast Louisiana (McBride, 1998; Omale and Lorenzo, 2015; Schuster, 1996). In the late

Cenozoic, Pliocene–Quaternary sedimentation and fault activity record uplift, climate change, and high-amplitude, high-frequency glacio-eustatic sea-level change within North America, as well as global climate change (Dokka et al., 2006; Ivins et al., 2007; Nunn, 1985).

METHODOLOGY

We conducted fault kinematic analysis on 140 faults within 11 published regional well-log cross sections (Bebout and Gutiérrez, 1982, 1983) and on six faults within four seismic reflection profiles in south Louisiana to determine the timing and magnitude of fault movement (Fig. 3; Figs. S1–S3¹). Fault kinematic analysis involves measuring cumulative throw (T), calculating incremental throw (ΔT ; Fig. 4),

¹Supplemental Material. Details on well log cross sections, seismic cross section, and LiDAR images within the study area. Please visit <https://doi.org/10.1130/GSAB.S.13369571> to access the supplemental material, and contact editing@geosociety.org with any questions.

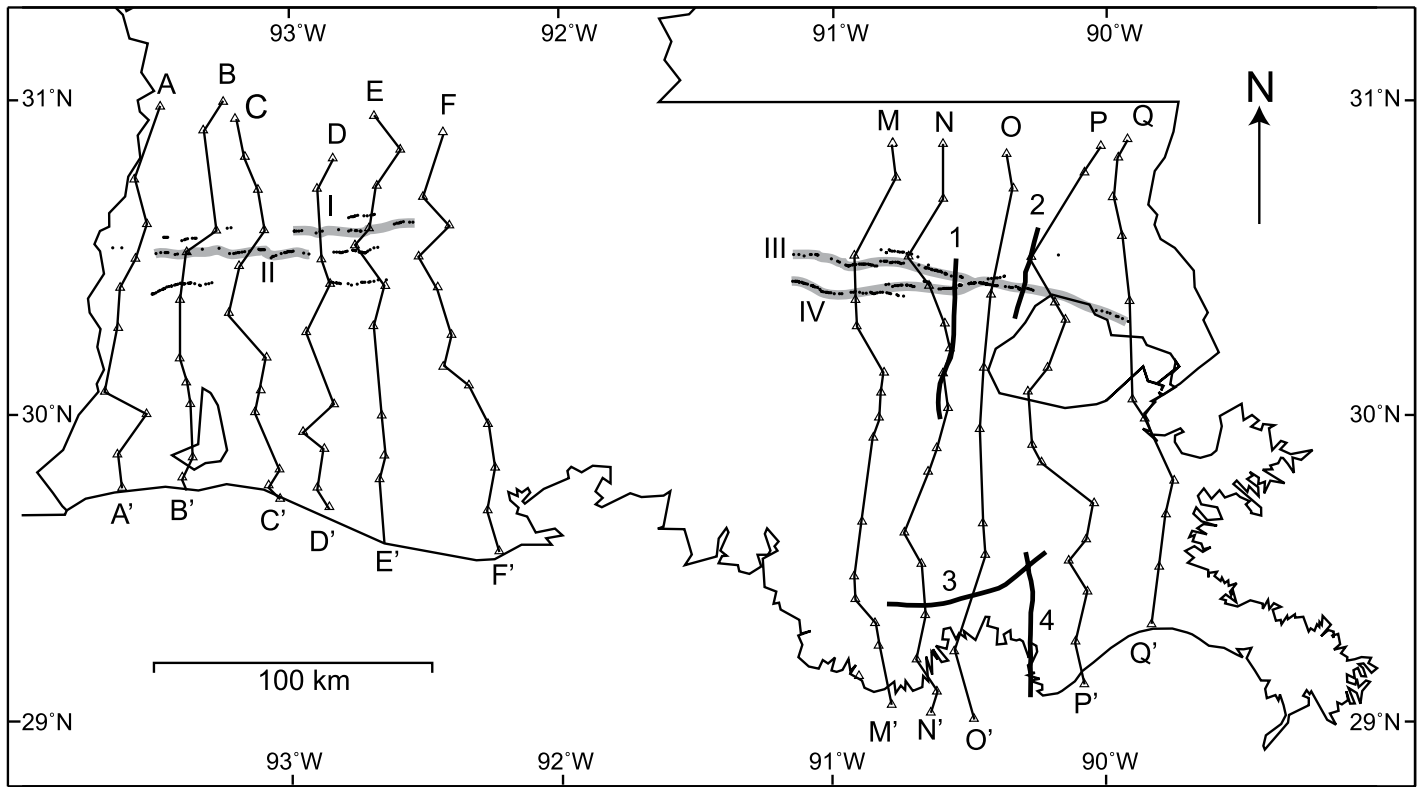


Figure 3. Location of well transects, seismic, and light detection and ranging (LiDAR) profiles in south Louisiana, United States, from which fault throws were measured. Triangles represent selected well locations along well transects (solid thin black lines; Bebout and Gutiérrez, 1982, 1983). Thick black lines numbered 1–4 are seismic lines. Black dots mark locations at fault scarps identified and measured from LiDAR data. Thick gray lines highlight offsets along the length of the fault scarps studied in this paper (Fig. 9). Data from southwest Louisiana are represented by well transects A–A’ through F–F’ (Fig. 6) and LiDAR profiles I and II (Fig. 9), while data from southeast Louisiana are represented by well transects M–M’ through Q–Q’ (Fig. 7), seismic lines 1–4 (Fig. 8), and LiDAR profiles III and IV (Fig. 9). Map projection is World Geodetic System 1984, World Mercator.

and making graphical representations in the form of incremental throw versus time ($\Delta T-t$) plots (Cartwright et al., 1998; Castellort et al., 2004; Mansfield and Cartwright, 1996). Cumulative throw is the total displacement of older horizons,

and it is the sum of several throw increments across a fault through time (Fig. 4; Figs. S1–S3). The horizons within the well-log cross sections are the tops of the major stratigraphic units that mark transgressive and regressive depositional

cycles in south Louisiana, identified by biostratigraphic and lithostratigraphic correlation (Figs. S1–S2; Bebout and Gutiérrez, 1982, 1983). To assign relative ages to seismic horizons (Fig. S3), we combined lithostratigraphic and biostratigraphic interpretations from nearby wells (McFarlan and LeRoy, 1988) with estimates of the depths to the tops of dated stratigraphic units from published regional structural maps, and thickness estimates from published isopach maps (Fisk, 1944; McFarlan and LeRoy, 1988; Rainwater, 1964). We note that the displacement estimates from well-log cross sections are technically “vertical separation,” although we use the term “throw” in order to maintain the “throw vs. time” and “throw vs. depth” terminology commonly used in the literature. Furthermore, actual throw will be greater than vertical separation for most faults in the study area because most of the strata (Tearpock and Bischke, 2003). However, we note that peak periods in sediment deposition will correlate with peak periods in both fault

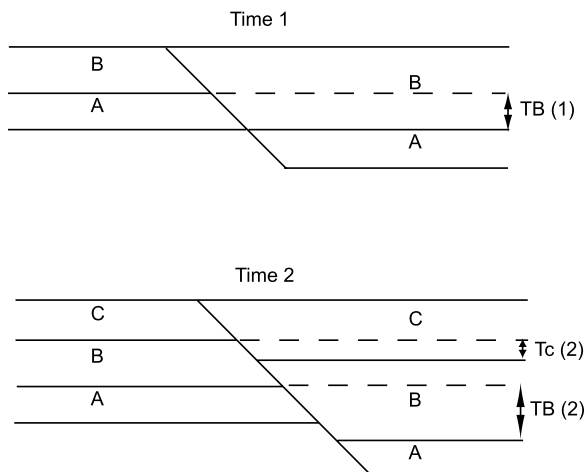


Figure 4. Method of determining incremental throw between two moments in time. At time 1, the top of unit A is offset by a cumulative throw $T_B(1)$. At time 2, the top of unit A is offset by a cumulative throw $T_B(2) = T_B(1) + T_C(2)$, and $T_B(2) \geq T_B(1)$. Original cumulative throw at time 1, $T_B(1) = T_B(2) - T_C(2)$.

throw and vertical separation if differential loading is a driving mechanism for salt mobilization and fault reactivation. This means that our comparison of changes in fault displacement with changes in sediment volumes remains valid, although the “throw” values estimated from the well-log cross sections may be underestimated.

To determine cumulative and incremental throw, we applied the “fill to the top assumption,” which implies that sedimentation completely fills the accommodation created by fault slip, leaving no persistent fault scarp after the deposition of sediments at any time (Fig. 4; Cartwright et al., 1998; Mansfield and Cartwright, 1996; Omale and Lorenzo, 2015). We also assumed that there was no erosion and no differential compaction between the footwall and hanging-wall blocks across faults. By assuming “fill to the top,” we interpreted that after the deposition of a stratigraphic unit, any additional displacement of the top of that unit occurred during subsequent sediment deposition, and the incremental throw was added to the throw of older units to produce a cumulative throw of the older units (Fig. 4). We calculated incremental throw by subtracting the throw of all younger horizons from older horizons (Fig. 4). Incremental throw values greater than zero were interpreted as periods of fault motion, while periods with zero incremental throw values were defined as periods of fault inactivity. We applied the “fill to the top” assumption to older Cenozoic periods (Paleocene–late Miocene/Pliocene) when the major sediment depositional centers were located in the present-day onshore south Louisiana, and sedimentation was most likely to surpass the accommodation space created by fault displacement. To graphically plot incremental throw against time, we assigned numerical ages to each formation in the well log and seismic cross sections from published stratigraphic charts (Fig. 5; Gradstein et al., 2012; Hackley, 2012).

We also analyzed the distribution, heights, and slopes of 500 fault line scarps identified in digital elevation maps constructed from LiDAR data (<http://atlas.lsu.edu/lidar>; Fig. 3; Fig. S4) to determine the most recent fault displacement. We extracted profiles perpendicular to the identified fault line scarps and used a smoothing function, defined based on the error function (Sandwell and Smith, 2005), to filter out topographic noise that could prevent direct measurements of the height and slope of the fault scarp. We also used a search function to find the best-fit height and slope from the smoothing function (Appendix 1). Relative ages of fault scarps were interpreted from the slopes of the scarps, with the assumption that younger fault scarps are steeper than older fault scarps because of shorter exposure to erosion, for scarps of the same height, similar deposits, and

under similar climatic conditions (Bucknam and Anderson, 1979; Enzel et al., 1994; Rao et al., 2017; Wallace, 1977). We note that the preservation of onshore fault scarps implies that the “fill to the top” assumption is not applicable to the most recent period of fault activity, which mainly correlates with a period of time during which the major sediment depocenter was located in the present-day offshore Gulf of Mexico.

Finally, we correlated changes in fault throw to changes in sediment supply during different periods of the Cenozoic. We drew on interpretations of changing tectonics and climate in source areas responsible for the changes in sediment supply to demonstrate that fault displacement history can record tectonic and climate signals in Earth history (Fig. 1).

RESULTS AND INTERPRETATION

The fault kinematic analysis revealed three peak periods of fault slip during the Cenozoic. Fault throw increased in the late Oligocene–early Miocene, middle Miocene–late Miocene, and Pleistocene. These peak periods correlated with a major increase in the rate of sediment supply and the development of new sediment depositional centers in south Louisiana, driven by tectonic and climatic forcing mechanisms in the sediment source areas within the interior of the North American continent (Figs. 6–10; Table 1; Tables S1–S17).

In southwest Louisiana, incremental throw along individual faults and average fault throw rates across all faults show that maximum fault slip took place in the late Oligocene–early Miocene (Fig. 6; Tables S1–S6). During this

period, a major increase in sediment supply rate, transported by a new fluvial axis (the Red River), formed a depocenter in the area (Fig. 2; Bentley et al., 2016; Galloway et al., 2011; Xu et al., 2017). The Red River connects tributaries that largely drain the elevated Colorado Plateau, Rocky Mountains, and Ouachita Mountains, as well as the remnant volcanic uplands of northern New Mexico during an arid climate (Cather et al., 2008; Chapin, 2008; Galloway et al., 2011), with warm and wet periods between 19 and 16 Ma (Fig. 10; Table 1; Retallack, 2007). In addition, locally, the Llano Uplift and uplift of the Edwards Plateau contributed sediments directly to the Gulf of Mexico, and the Edwards Plateau deflected an existing river to connect with the Red River, providing additional sediments during this period (Galloway et al., 2011; Xu et al., 2017). Consequently, the loading caused by deposition of large volumes of sediment displaced significant volumes of salt, forming salt withdrawal minibasins and growth faults (Diegel et al., 1995; Peel et al., 1995).

In southeast Louisiana, incremental throw estimates show that a major increase in fault displacement began in the early Miocene and continued through the late Miocene (Figs. 7, 8, and 10; Table 1; Tables S7–S17). These maximum values are an order of magnitude greater than those estimated for previous periods. This major increase in sediment supply was concomitant with the increase in fault displacement, especially for the middle to late Miocene. During the middle Miocene, a new fluvial axis, the paleo-Tennessee River, transported sediment into southeast Louisiana and developed a new sediment depocenter (Fig. 2; Galloway et al.,

Era	Period	Epoch	Stratigraphic Unit	Age (Ma)	
Cenozoic	Neogene	Pliocene	Pliocene	2.6	
		Miocene	Upper Miocene	5.3	
			Middle Miocene	11.6	
			Lower Miocene	15.9	
	Paleogene	Oligocene	Anahuac Fm.	23	
			Frio Fm.	25	
			Vicksburg Grp.	28	
		Eocene	Jackson Grp.	33.9	
			Cockfield/Yegua Fms.	37	
			Sparta Fm.	42	
			Wilcox Grp.	47.8	
		Paleocene	Midway Grp.		59.2
					65

Figure 5. Stratigraphic units identified in well-log cross sections (Hackley, 2012). The tops of these units define stratigraphic markers for fault throw measurement (Figs. 6–7; Tables S1–S11 [see text footnote 1]). Fm.—Formation, Grp.—Group.

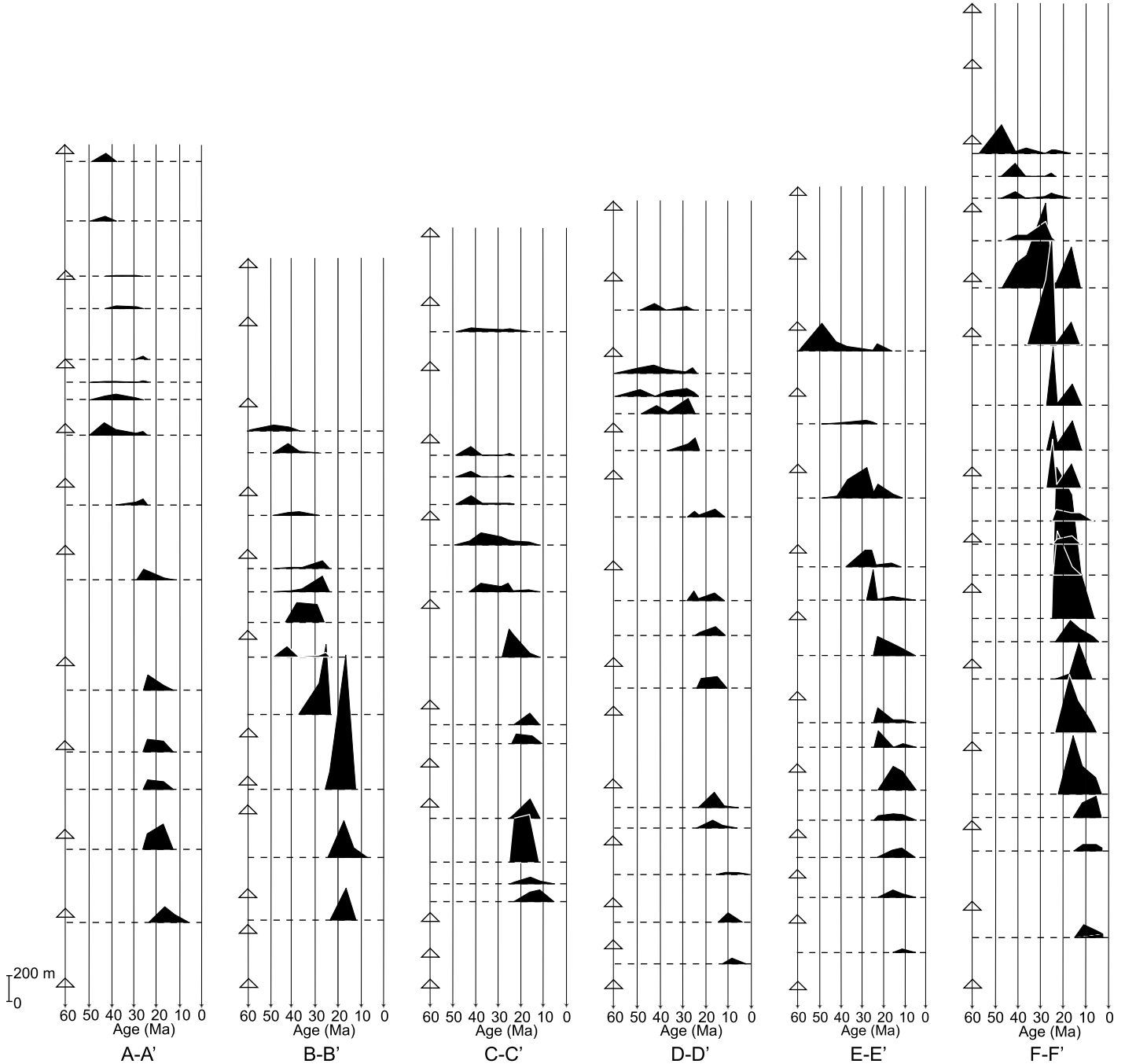


Figure 6. Incremental fault throw vs. time plots for cross sections A–A’ to F–F’, southwest Louisiana (Tables S1–S6 [see text footnote 1]; see Fig. 3 for location). Fault throw from the top to bottom of each stack is from faults identified from north to south in each cross section. Open triangles on the left of each stack, from top to bottom, correspond to the well locations (triangles) in Figure 3, from north to south. Highest points on polygons represent maximum incremental fault throw for that period. Fault throw is highest in the early Miocene in southwest Louisiana. Fault throw measurements (edges of each polygon) are absent for periods with a dashed line on either side of the polygon (Tables S1–S6). Incremental fault throw is zero, i.e., fault inactivity, for periods where there is a dashed base line between polygons.

2011). The paleo–Tennessee River became a dominant transport agent and increased sediment supply either because of increased storm intensity in the Appalachians, related to a change to cooler and climatic conditions (Boettcher and Milliken, 1994; Galloway et al., 2011), and/or

epeirogenic uplift of the Appalachian Mountains (Fig. 10; Table 1; Bentley et al., 2016; Fernandes et al., 2019; Gallen et al., 2013; Liu, 2014, 2015; Miller et al., 2013; Pazzaglia and Brandon, 1996). Since the Miocene, increases in sediment supply led to significant salt evacuation and

growth faulting in southeast Louisiana, forming prominent salt basins, e.g., the Terrebonne Trough (Diegel et al., 1995; McBride, 1998; Peel et al., 1995; Schuster, 1996).

A comparison of fault throw between southwest and southeast Louisiana showed that the

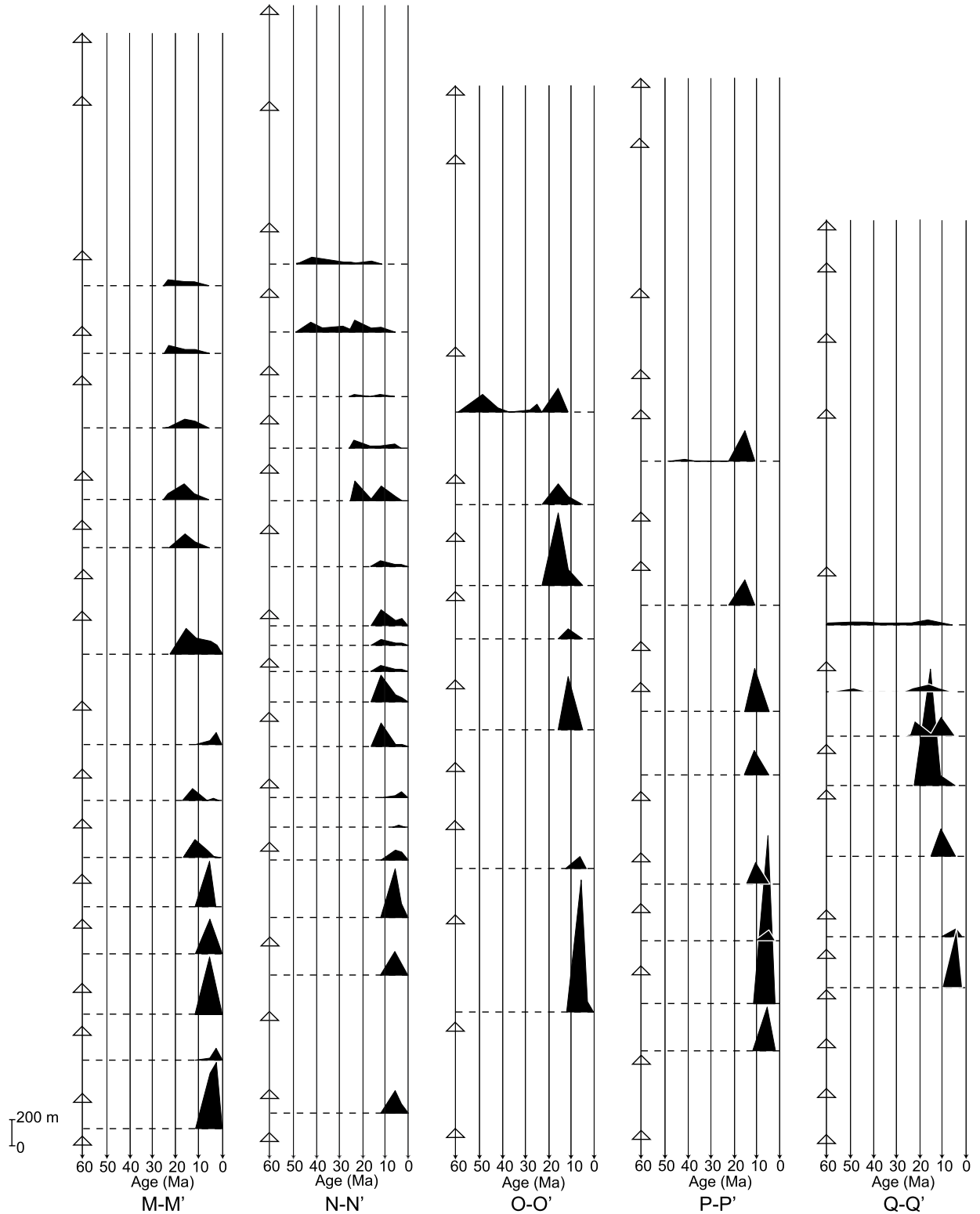


Figure 7. Incremental fault throw vs. time plots for cross sections M-M' to Q-Q', southeast Louisiana (Table S7-S11 [see text footnote 1]; see Fig. 3 for location). Fault throw from the top to bottom of each stack is from faults identified from north to south in each cross section. Open triangles on the left of each stack, from top to bottom, correspond to the well locations (triangles) in Figure 3, from north to south. Highest points on polygons represent maximum incremental fault throw for that period. Fault throw is highest in the late Miocene in southeast Louisiana. Fault throw measurements (edges of each polygon) are absent for periods with a dashed line on either side of the polygon (Tables S7-S11). Incremental fault throw is zero, i.e., fault inactivity, for periods where there is a dashed base line between polygons.

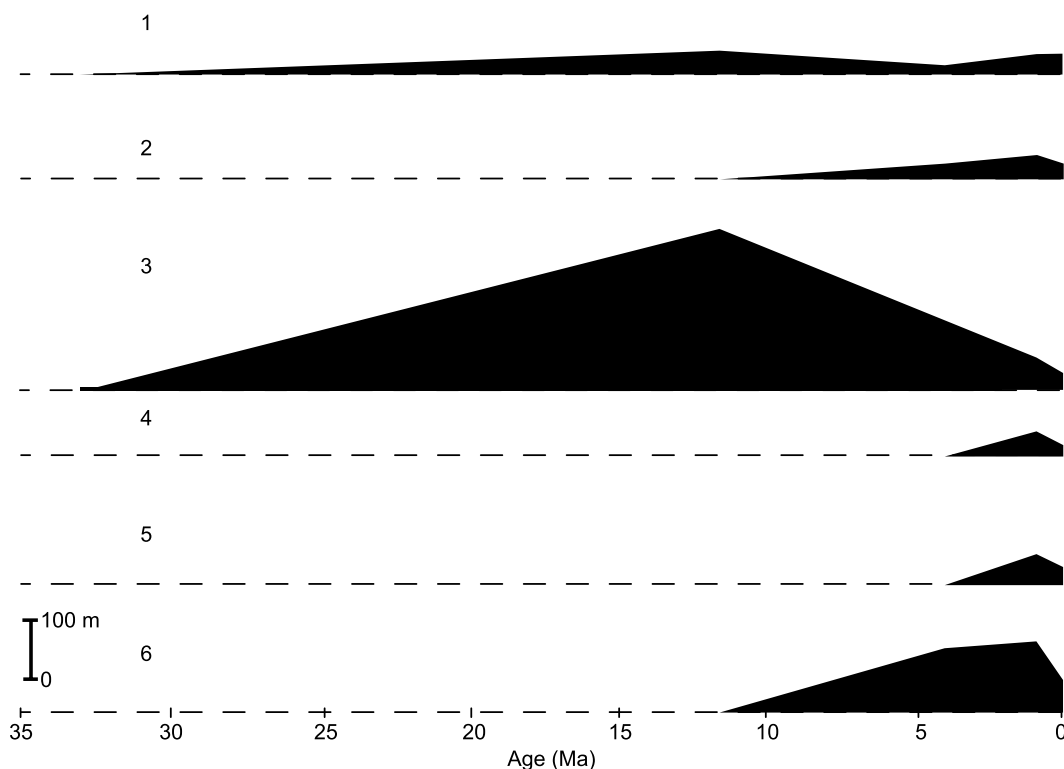


Figure 8. Fault throw vs. time measured from faults identified in seismic sections from southeast Louisiana (see Fig. 3 for location). Fault throw is highest in the Miocene. Plots 1–3 represent faults identified from north to south along seismic profile 1, and plots 4, 5, and 6 are faults identified within seismic profiles 2, 3, and 4, respectively. Dashed horizontal lines represent zero fault throw. For each fault plot, there are no available throw measurements on stratigraphic units represented by the periods without polygons.

timing and amount of fault slip records a temporal shift in the location of maximum fault displacement from southwest to southeast Louisiana during the Cenozoic. Incremental throw maxima, which correlate with major depocenter activity, are higher in the east (average incremental throw of 335 m) than in the west (average incremental throw of 180 m; Figs. 6, 7, and 10; Table 1; Tables S1–S17). This possibly reflects the availability of more salt or an overall greater sediment supply during the middle–late Miocene in the east during peak sedimentation than during the Oligocene–early Miocene depocenter development in the west. Overall, the west-to-east shift correlates with a similar shift in dominant sediment source, from the Rocky Mountains in the west to the Appalachians in the east, as well as shifts in the loci of sediment deposition and salt evacuation in south Louisiana (Figs. 2 and 10; Table 1). Sediment supply into southwest Louisiana from the Rocky Mountains decreased because of early Miocene regional subsidence in surrounding interior areas that reduced stream gradients (Bentley et al., 2016; McMillan et al., 2006) during an increasingly arid climate (Zachos et al., 2001) in that region (Bentley et al., 2016; Chapin, 2008; Galloway et al., 2011). Although increasing aridity may increase the frequency of large flooding events and consequently the volume of coarse sediment transported downstream (Molnar, 2001), regional subsidence dominated in the western

United States, associated with Rio Grande rifting and Basin and Range extension. This led to reduced sediment supply to the Gulf of Mexico from the western interior, as interior basins captured more sediments (Bentley et al., 2016; Galloway et al., 2011; Xu et al., 2017).

The fault throw estimates show that major fault reactivation migrated southward with time (Figs. 6–7; Tables S1–S11), correlating with the progradation of deltaic sediments since the Cenozoic (Fig. 2). Sediment progradation depends on the interplay between sediment supply and relative sea level, in the absence of additional subsidence mechanisms that can create accommodation space (Klotsko et al., 2015; Posamentier et al., 1988; Rasmussen, 2004; Vail et al., 1977; Van der Zwan, 2002). During most of the Cenozoic, sediment supply in the Gulf of Mexico dominated over sea-level changes to allow continuous deltaic progradation, with significant increases in sediment supply in the Paleocene, Miocene, and Pleistocene (Bentley et al., 2016; Galloway, 2008; Galloway et al., 2005, 2011). For example, during the Miocene, between 23 Ma and 5 Ma, fault reactivation shifted southward in time in southeast Louisiana (Fig. 7). During this period, sediment supply increased, and the deltaic depocenters prograded southward from their previous positions (Fig. 2). However, global sea-level estimates show an increase (<50 m) in sea level from Oligocene values during the early and middle Miocene

(Haq et al., 1987; Vail et al., 1977). Typically, this sea-level rise would be predicted to have negatively affected progradation, driving shoreline retreat. In contrast, increases in sediment supply from the Appalachians since the Miocene in response to an increase in mantle-driven surface topographic relief (Gallen et al., 2013; Liu, 2014; Miller et al., 2013), coupled with late Miocene increases in precipitation and seasonality in response to climatic cooling (Boettcher and Milliken, 1994; Galloway et al., 2011), dominated over the sea-level rise. Furthermore, sea level may have fallen in the late Miocene (Haq et al., 1987; Vail et al., 1977), which would favor coastal progradation with a steady rate of, or an increase in, sediment supply. Alternatively, sea level was relatively constant throughout the Miocene (Miller et al., 2005, 2011, 2020), and deltaic progradation and the southward migration of peak fault activity in the Gulf of Mexico during this period mainly reflect the increase in sediment supply from the Appalachians. We note that the interpretation of a southward migration of peak fault throw with time may be biased by the fewer or indeed lack of fault throw estimates for older time periods in the southern part of the study area (Tables S7–S11). There are fewer fault throw estimates for older periods in the southern part of the study area because these older units are deeply buried by the younger sediments, beyond the maximum depth of penetration of the well logs (Fig. S1). However, we would expect

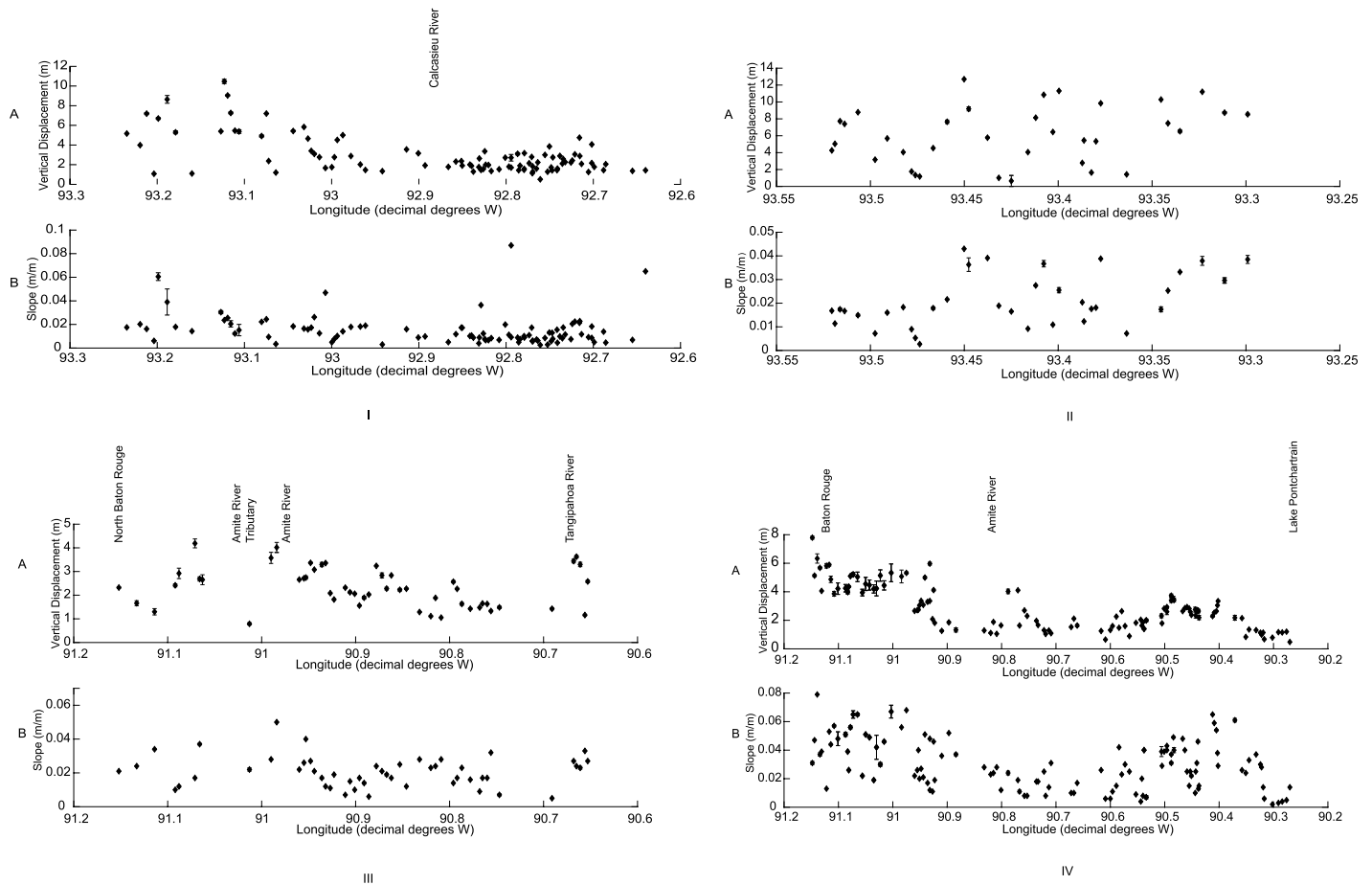


Figure 9. (A) Vertical offsets and (B) slopes from fault scarps within light detection and ranging (LiDAR) profiles (see Fig. 3 for location). Heights (vertical displacement) and slopes of fault scarps are higher toward the western part of south Louisiana.

the correlation between fault throw and sediment supply that we observed in areas where data are available to continue for these older time periods, because we infer that the mechanism for salt displacement and fault reactivation remained the same within the basin.

Fault throw estimates for both southwest and southeast Louisiana show that fault inactivity ($\Delta T = 0$) occurred mostly during the Eocene (Figs. 6–7), a period marked by a lower sediment supply by the Mississippi River and a shift in major sedimentation to central Louisiana (Fig. 2; Galloway et al., 2011). The reduced sediment supply resulted from reduced runoff in the northern Rocky Mountains caused by increasing aridity and drainage reorganization (Table 1; Davis et al., 2009; Sewall and Sloan, 2006; Wilf, 2000). The development of a broad lowland in the central United States, caused by dynamic subsidence associated with the eastward motion of the Farallon slab, may have aided this drainage reorganization and the capture of sediments by interior basins, leading to reduced Eocene sediment supply to the Gulf of Mexico (Liu,

2014, 2015). In addition, globally high sea levels may have combined with the low sediment supply to cause transgression of the northern Gulf of Mexico onto the Eocene shelf (Bentley et al., 2016; Galloway et al., 2011).

The fault throw estimates show fault reactivation in both southwest and southeast Louisiana during the Pleistocene (Fig. 8; Tables S12–S19). During this period, the depocenter extended across south Louisiana, fed by three main fluvial axes (Fig. 2; Bentley et al., 2016; Galloway et al., 2011; Saucier, 1994; Thompson, 1991). The wide extent of the depocenter and increase in sediment supply in the Pleistocene occurred in response to the advance and retreat of ice sheets during the North American glaciation, coupled with epeirogenic uplift in the western interior since the Pliocene (Fig. 10; Table 1). The heights and slopes of fault scarps, which constrain the fault displacement history of the Pleistocene and Holocene strata across south Louisiana, decrease from southwest Louisiana (average height of 4–12 m) to southeast Louisiana (average height <4 m; Fig. 9; Tables S18–S19). However, fault

scarp slopes are below an average of 0.04 m/m in south Louisiana, except in the Baton Rouge area (southeast Louisiana), where slopes reach as high as 0.08 m/m (Fig. 9; Tables S18–S19). This suggests that the steeper-sloped faults in the Baton Rouge area were active more recently than the faults in the western part of south Louisiana, following the methods of interpreting fault scarp age based on slopes (Bucknam and Anderson, 1979; Enzel et al., 1994; Rao et al., 2017; Wallace, 1977). Another reason to suggest a different age for the fault scarps is that, for scarps of the same age but different resistance to erosion, the scarps in more resistant material will have steeper slopes than those in less resistant material. Following that interpretation, the Baton Rouge area, which is covered by loess (Heinrich, 2008), a more easily erodible material, might be expected have gentler slopes than southwest Louisiana if the scarps were the same age. It is important to note that the Pleistocene fault displacements from fault scarps represent an underestimate of the actual fault throw, because the major salt displacement

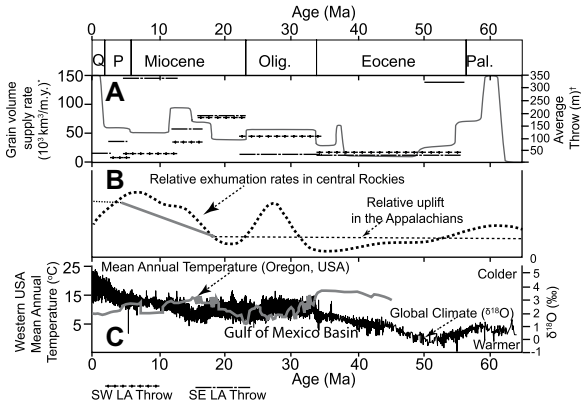


Figure 10. Fault throws for southwest Louisiana (SW LA) were greatest in the Oligocene (Olig.) to early Miocene sections, when exhumation rates increased in the central Rockies (Clift, 2010) and when the western United States experienced a warm and wet climatic period. Mean annual temperature was determined using paleosols in Oregon (Retallack, 2007). Global climate was determined from $\delta^{18}\text{O}$ (Zachos et al., 2001).

In comparison, fault throws in southeast Louisiana (SE LA) were highest during the time of uplift of the Appalachians (Gallen et al., 2013; Miller et al., 2013). Sedimentation rates (Galloway et al., 2011) were highest during the Paleocene, Miocene, and Quaternary. Quaternary (Q) glaciations may relate to the most recent fault activation detected on surface faults in the study area (Fig. 9), and offshore Louisiana, out of the study area. Note that although exhumation rates increased in the central Rockies in the middle–late Miocene, regional subsidence associated with the Rio Grande Rift and Basin and Range captured sediments and led to reduced sediment supply to the Gulf of Mexico. *Grain volume sediment supply rate (Galloway et al., 2011) is for the entire northern Gulf of Mexico, including additional drainage axes and depocenters west and east of the study area. †Average throw values may be affected by the few number of, or lack of, fault throw measurements for some periods (Tables S1–S17 [see text footnote 1]), because some horizons were not sampled by the minimum or the maximum depth of the well logs or seismic data (Figs. S1–S3 [see text footnote 1]). Fault throw from light detection and ranging (LiDAR) (Fig. 9; Table 1) is not plotted. P—Pliocene; Pal.—Paleocene.

and fault displacement in response to Pleistocene sediment loads are now located offshore Louisiana, i.e., the location of the Pleistocene sediment depocenter (Fig. 2), and the well-log and seismic surveys in this study did not cover that area. By the Pleistocene, deltaic progradation that started in the Paleocene, coupled with increased sediment supply in response to Pleistocene glaciation, had caused the major sediment depocenters to migrate south into present-day offshore Gulf of Mexico (Fig. 2). Studies in the Gulf of Mexico have documented extensive salt evacuation and fault reactivation in the Pleistocene (Diegel et al., 1995; Peel et al., 1995; Schuster, 1996).

DISCUSSION

Fault kinematic analysis can be used to identify and quantify previously unmapped volumes of sediment (Fig. 11). For example, prior work indicates that the first Cenozoic depocenter in southeast Louisiana formed in the middle Miocene (Galloway et al., 2011). However, in the early Miocene, fault throws increased significantly across south Louisiana (Figs. 6–7) and imply an increase in sedimentation rate in that area. In particular, increased salt withdrawal caused by differential loading might have

TABLE 1. TECTONICS, CLIMATE, AND AVERAGE FAULT THROW FOR THE GULF OF MEXICO

Age (Ma)	North American tectonics				North American climate				Global climate (Zachos et al., 2001)
	Rocky Mountains and Great Plains	SW LA throw* (m)	Appalachians	SE LA throw (m)	Rocky Mountains	SW LA throw (m)	Appalachians	SE LA throw (m)	
Pleistocene (0)	Broad domal epeirogenic uplift Tilting of Western High Plains (1,4,5,6)	15	High elevation (1)	86.64	Cool to cold; ice-sheet advance and retreat (1,2)	4†	Cool to cold; ice-sheet advance and retreat (1,2,3)	3†, 35‡	Cooler than Pliocene
Pliocene (2.59)	High Plains (1,4,5,6)	15	Broad uplift (1,8,9,10,11)	86.64	Cool, temperate; monsoonal, subarid (1,2,7)		Cool, temperate (1)		Cooler than Miocene
Late Miocene (5.33)	Slow regional and local extension and subsidence (1,4,8)	32		335	Cooler, drier, less variable than middle Miocene, arid (7,8)		Cooler, drier, less variable than middle Miocene, temperate (1,8)		Onset of cooling
Middle Miocene (11.6)		82		133	Warm, temperate (1,7,12)		Warm, wet, temperate; increased storm intensity (1,8,11,13)		Mid-Miocene climatic optimum
Early Miocene (15.97)		180	Possible uplift beginning at 18 Ma (9,10)	180	Warm, wet, seasonal aridity continued from Oligocene (1,7,14,15)		Warm, temperate (1,8)		Warm
Oligocene (23.03)	Regional thermally driven uplift (1)	102	Quiescent (1)	31	Dry, cool, subarid to arid (1)		Temperate (1)		Late Oligocene warming; Oligocene glaciation
Eocene (33.9)		40	Quiescent (1)	25	Variable in time; warm subarid to warm temperate to subarid/arid (1,16,17)		Warm to cool, temperate (1)		Less warm in Middle and late Eocene; early Eocene climatic optimum

Note: Pliocene and Pleistocene fault throw may be underestimated because the main sediment depositional centers and major salt displacement during these periods are now located offshore Louisiana. Source-area tectonic and climatic events control sediment supply to the Gulf of Mexico, as indicated by average fault throw and global climate during the same period. Southwest Louisiana source area is the Rocky Mountains and Great Plains, whereas southeast Louisiana source area is the Appalachian Mountains. The west-to-east shift in higher fault throw in the Miocene was a consequence of a west-to-east shift in the location of maximum sediment supply, caused by the uplift of the Appalachians. References: 1—Galloway et al. (2011); 2—Thompson (1991); 3—Saucier (1994); 4—McMillan et al. (2006); 5—Eaton (2008); 6—McMillan et al. (2002); 7—Chapin (2008); 8—Bentley et al. (2016); 9—Miller et al. (2013); 10—Gallen et al. (2013); 11—Pazzaglia and Brandon (1996); 12—Boettcher and Milliken (1994); 13—Retallack (2007); 14—Cather et al. (2008); 15—Wilf (2000); 16—Davis et al. (2009); 17—Sewall and Sloan (2006).

*Pliocene fault throw estimates for southwest Louisiana may be affected by insufficient data because only two measurements were used in calculating the average throw. This is because the well logs used in this study begin at 3000 ft (914 m), below the Pliocene unit.

†Fault throw measured from light detection and ranging (LiDAR) profiles.

‡Fault throw measured from seismic cross sections. All other fault throw values are from well-log cross sections (see Fig. 3 for locations).

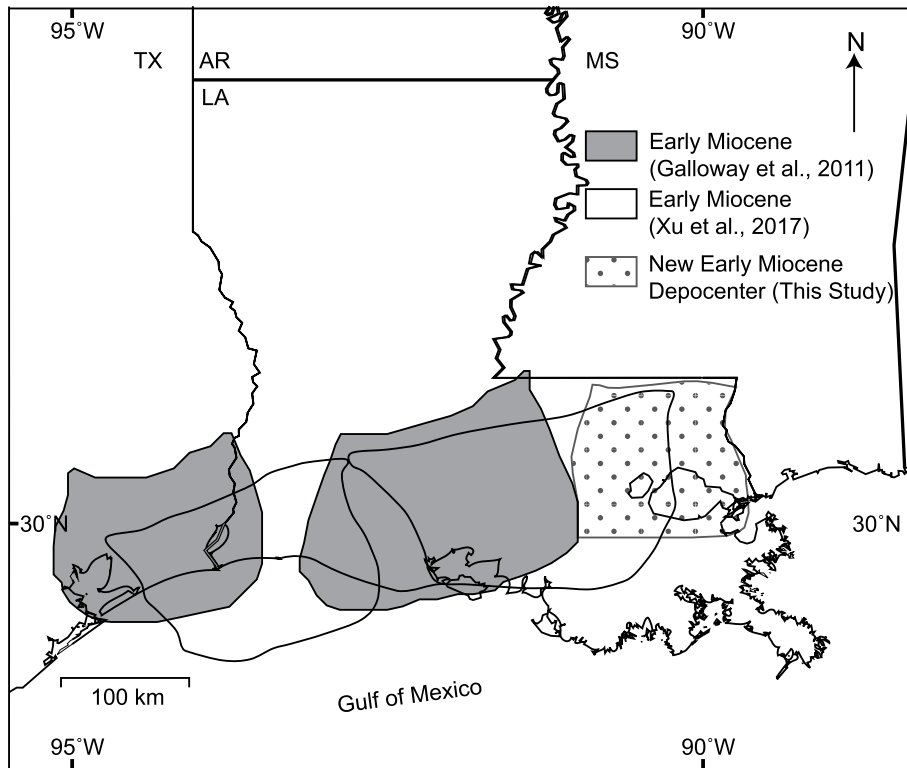


Figure 11. New early Miocene depocenter identified in this study from fault kinematic analysis extends early Miocene depocenter further east, beyond original eastern limit (Galloway et al., 2011) and modified eastern limit (Xu et al., 2017). Note that the limit of the depocenter proposed in this study is based on data coverage, and early Miocene depocenter may extend beyond the mapped location in this study, including beyond the southern boundary. Map projection is World Geodetic System 1984, World Mercator. See Figure 2 for state abbreviations.

been a driving mechanism for fault movement (Diegel et al., 1995; McBride, 1998; Omale and Lorenzo, 2015; Peel et al., 1995; Schuster, 1996; Thorsen, 1963). Early Miocene depocenters are documented across the region, but only for southwest and south-central Louisiana (Galloway et al., 2011). There is some evidence of a possible early Miocene increase in sediment supply to the area if we assume that the paleo-Tennessee River was already a dominant sediment supplier in the early Miocene. This would have brought sediments from the Appalachian Mountains. Studies of topographic relief and river profile knickpoints in the Cullasaja Basin of the Appalachian Mountains show that epeirogenic uplift of the landscape and increase in relief (~150%) may have begun as early as ca. 18 Ma (Gallen et al., 2013). A possible mechanism for this epeirogenic uplift in the southern Appalachians is isostatic response to delamination of the Farallon slab, supported by the spatial correlation between uplifted regions and lithospheric geophysical anomalies, interpreted as relict slab fragments (Gallen et al., 2013). Alternatively, numerical simulations of buoyancy-

induced mantle flow, associated with the sinking of the Farallon slab, suggest that dynamic subsidence caused tilting of the North American continent and enhanced differential erosion within the Appalachians by 15 Ma (Liu, 2014). Increased erosion led to an increase in sediment supply to the Gulf of Mexico and eastern North American margin, and flexural isostatic adjustments in response to this enhanced differential erosion created up to 400 m of relief and 200 m of surface uplift since the Miocene (Liu, 2015). It is well established that epeirogenic uplift has affected the Appalachian Mountains in the southeast United States and caused increases in sediment supply to the northern Gulf of Mexico, at least by the middle Miocene (Bentley et al., 2016; Boettcher and Milliken, 1994; Galloway, 2008; Galloway et al., 2011). The estimated increase in fault throw rates favors an increase in early Miocene sediment input to southeast Louisiana at this time, transported by the paleo-Tennessee River and triggered by Appalachian uplift. Alternatively, the previously mapped early Miocene depocenter (Galloway et al., 2011; Xu et al., 2017) fed by the paleo-Mississippi River

would have extended further east of the previously mapped location (Fig. 11).

Fault throw estimates within passive margins can also indicate periods of high sediment supply despite partial later erosion of the sediments (Fig. 12). Our fault kinematic analysis from the Gulf of Mexico shows that fault throw correlates with spatial and temporal changes in sediment volumes within the depocenter. We suggest that this relationship may be typical of overfilled sedimentary basins where underlying mobile substrates such as salt or shale are displaced. Fault throw will be higher during periods of higher sediment supply and vice versa at such passive margins. We further infer that because changes in fault throw correlate with changes in sediment supply within these overfilled sedimentary basins, fault throw can record missing sediment volumes. This is because fault offsets can be preserved in the rock record despite partial erosion if erosion does not remove material from the footwall. For example, if a fault displaces a sedimentary unit in response to deposition of sediment loads that surpass accommodation (Fig. 12, time 1), and subsequently some sediments are eroded, but the footwall is preserved, then the fault throw is also preserved (Fig. 12, time 2). If, at a later time, an incremental fault displacement (T_c) occurs (Fig. 12, time 3), then the initial fault throw across the older unit increases and is added to the cumulative fault throw (T_B). The initial fault throw (T_0), which results from the deposition of the larger sediment volume at time 1 that is now partially eroded by time 2 (Fig. 12), can still be estimated from the most recent cross section (Fig. 12, time 3). By using fault kinematics to evaluate missing sediment volumes, greater fault throw can be linked to greater sediment supply and then linked to the relative changes in the magnitude of tectonic and/or climate-related processes driving changes in sediment supply. An example of a passive margin where fault kinematics may be used to evaluate missing sediment volumes and the magnitude of tectonic and climatic changes is the West African Congo margin, a salt-bearing passive margin with fault activity and extensive early Miocene erosion (Anka et al., 2010; Lavier et al., 2001; Walgenwitz et al., 1992).

CONCLUSIONS

We combined kinematic analysis of 146 faults identified in well-log and seismic data with the analysis of the height and slope distribution of fault scarps onshore in the northern Gulf of Mexico. Fault throw increased contemporaneously with the development of Cenozoic depositional centers in space and time in south Louisiana. In the early Miocene, fault throw increased in

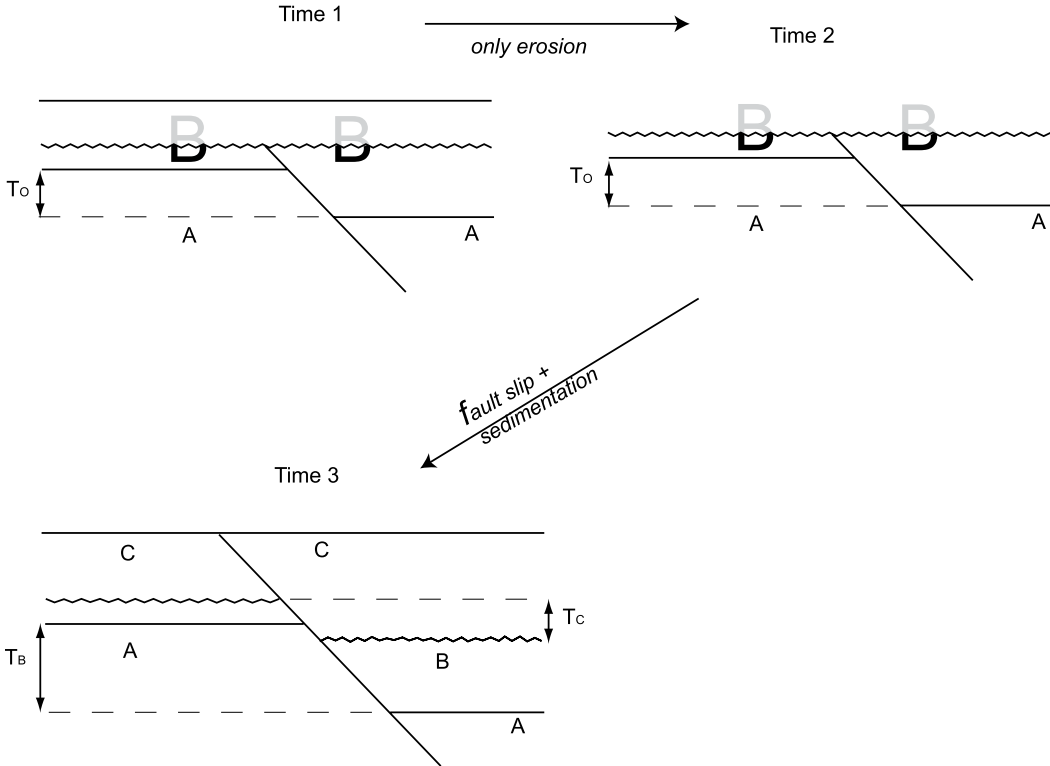


Figure 12. Conceptual sketch of how fault throw may be preserved despite partial erosion of sediments. Although unit B is partially eroded by time 2, the initial throw before erosion, T_0 , formed by the end of time 1 remains the same during both periods. With incremental throw T_C in time 3, the cumulative throw offsetting the top of unit A is $T_B = T_0 + T_C$. The throw at time 1 that was preserved at time 2 can be calculated from the cumulative throw at time 3.

southwest Louisiana, as increased runoff from the elevated Rocky Mountains and volcanic uplands of New Mexico increased sediment supply and supplied a new depocenter. In the middle and late Miocene, fault throw increased in southeast Louisiana, when a new depositional center formed in that area. This new depocenter developed because epeirogenic uplift and increased storm intensity in the Appalachian Mountain region increased sediment supply to the area. The Eocene fault record shows the most fault inactivity and the least amount of fault reactivation in southwest and southeast Louisiana, because the depocenter was in central Louisiana during this period. Increasing aridity and drainage reorganization in the northern Rocky Mountain region led to lower sediment supply rates. When combined with globally high sea levels, this restricted the depocenter to central Louisiana. By correlating fault throw with sediment supply and depocenter location, we infer that fault throw can be a proxy for the spatial and temporal locations of the depocenter, as well as the tectonic and climatic activities that controlled sediment supply.

Our careful analysis of fault throw indicates that a previously mapped early Miocene depocenter would have extended further east into southeast Louisiana. Differential loading is the preferred mechanism interpreted to have caused this fault displacement.

We suggest that fault kinematic analysis can be used to interpret tectonic and climatic con-

trols on sedimentation at other passive margins affected by gravitational tectonics. We also infer that fault throw estimates can indicate missing sediment volumes and the relative magnitudes of tectonic and climatic processes that drive changes in sediment supply at these margins. This inference is possible because fault throw estimates can be preserved despite partial erosion of sediments, allowing previously unconstrained rates of sedimentation to be partially estimated.

APPENDIX 1. AUTOMATIC FITTING OF TOPOGRAPHIC PROFILES

A best fit of topographic profiles, oriented perpendicular to fault line scarps, can help to filter short-wavelength topographic noise and provide an automatic way to measure the height and slope of the fault scarp. We used an error function template to best match the shape of the scarp profile:

$$F(x) = -A * erf(u) + B, \tag{1}$$

where A is the slope of the function $F(x)$, and B is its intercept. In the error function

$$erf(u) = \frac{2}{\sqrt{\pi}} \int_0^u e^{-(\xi)^2} d\xi, \tag{2}$$

ξ is a dummy variable, and $u = (X - X_0)C$ is used to calculate height at different horizontal positions (X) away from the location of the scarp (X_0), where C is related to the slope (Fig. A1).

Figure A1. The original profile (dashed red) and its best fit (solid blue).

Both A and B in Equation 1 are linear for any value of C and X_0 . We first wrote a search function in MATLAB to find convenient starting values for C and X_0 by minimizing the following objective function and iterating through a predetermined range of realistic values for C and X_0 :

$$D = \frac{\left(\sum (y - \bar{y}) * (erf(u) - \overline{erf(u)}) \right)^2}{\left(\sum erf(u) - \overline{erf(u)} \right)^2}, \tag{3}$$

where y and \bar{y} are the original data and their mean, respectively. For general values of C and X_0 , and when the error function cannot fully develop across data sets of finite lateral extent, its mean, $(erf(u))$, may be nonzero.

By obtaining the values of C and X_0 , the optimum values of A and B can be found by linear regression:

$$A = \frac{\sum (erf(u) - \overline{erf(u)})(y - \bar{y})}{\sum (erf(u) - \overline{erf(u)})^2}, \tag{4}$$

$$B = A * erf(\bar{u}) + \bar{y}, \tag{5}$$

where y is the original scarp height.

The error associated with the best-fit line is the root mean square (RMS) error. The RMS error is the square root of the average of the squared residual. The residual of the best fit is the difference between the original data (the topographic profile) and the best fit (the error function):

$$RMS = \sqrt{\frac{\sum (y - erf(u))^2}{n}}, \tag{6}$$

where n is the number of samples in y .

ACKNOWLEDGMENTS

We thank the two reviewers and associate editor for critical reviews and constructive feedback on the original manuscript.

REFERENCES CITED

Anka, Z., Séranne, M., Lopez, M., Scheck-Wenderoth, M., and Savoye, B., 2009, The long-term evolution of the Congo deep-sea fan: A basin-wide view of the interaction between a giant submarine fan and a mature passive margin (ZaiAngo project): *Tectonophysics*, v. 470, no. 1–2, p. 42–56.

Bebout, D.G., and Gutiérrez, D.R., 1982, Regional Cross Sections, Louisiana Gulf Coast, Western Part: Louisiana Geological Survey Folio 5, 11 p.

Bebout, D.G., and Gutiérrez, D.R., 1983, Regional Cross Sections, Louisiana Gulf Coast, Eastern Part: Louisiana Geological Survey Folio 6, 10 p.

Bentley, S., Blum, M., Maloney, J., Pond, L., and Paulsell, R., 2016, The Mississippi River source-to-sink system: Perspectives on tectonic, climatic, and anthropogenic influences, Miocene to Anthropocene: *Earth-Science Reviews*, v. 153, p. 139–174, <https://doi.org/10.1016/j.earscirev.2015.11.001>.

Blum, M., and Pecha, M., 2014, Mid-Cretaceous to Paleocene North American drainage reorganization from detrital zircons: *Geology*, v. 42, no. 7, p. 607–610, <https://doi.org/10.1130/G35513.1>.

Boettcher, S.S., and Milliken, K.L., 1994, Mesozoic–Cenozoic unroofing of the southern Appalachian Basin: Apatite fission track evidence from middle Pennsylvanian sandstones: *The Journal of Geology*, v. 102, no. 6, p. 655–668, <https://doi.org/10.1086/629710>.

Brun, J.-P., and Fort, X., 2011, Salt tectonics at passive margins: Geology versus models: *Marine and Petroleum Geology*, v. 28, no. 6, p. 1123–1145, <https://doi.org/10.1016/j.marpetgeo.2011.03.004>.

Bucknam, R., and Anderson, R., 1979, Estimation of fault-scarp ages from a scarp-height–slope-angle relationship: *Geology*, v. 7, no. 1, p. 11–14, [https://doi.org/10.1130/0091-7613\(1979\)7<11:EOFAFA>2.0.CO;2](https://doi.org/10.1130/0091-7613(1979)7<11:EOFAFA>2.0.CO;2).

Buffler, R.T., Thomas, W.A., and Speed, R., 1994, Crustal structure and evolution of the southeastern margin of North America and the Gulf of Mexico basin, in Speed, R.C., ed., *Phanerozoic Evolution of North American Continent–Ocean Transitions*: Boulder, Colorado, Geological Society of America, *Geology of North America, Continent–Ocean Transect Summary Volume*, p. 219–264, <https://doi.org/10.1130/DNAG-COT-PEN.219>.

Busby, C.J., Ingersoll, R.V., and Burbank, D., 1995, *Tectonics of Sedimentary Basins*: Oxford, UK, Blackwell Science Oxford, 579 p.

Busby, C.J., Busby, C., and Azor, A., 2012, Extensional and transtensional continental arc basins: Case studies from the southwestern United States, in Busby, C., and Azor, A., eds., *Tectonics of Sedimentary Basins: Recent Advances*: New York, John Wiley and Sons, p. 382–404.

Cartwright, J., Bouroulec, R., James, D., and Johnson, H., 1998, Polycyclic motion history of some Gulf Coast growth faults from high-resolution displacement analysis: *Geology*, v. 26, no. 9, p. 819–822, [https://doi.org/10.1130/0091-7613\(1998\)026<0819:PMHOSG>2.3.CO;2](https://doi.org/10.1130/0091-7613(1998)026<0819:PMHOSG>2.3.CO;2).

Castellort, S., Pochat, S., and Van Den Driessche, J., 2004, Using T-Z plots as a graphical method to infer lithological variations from growth strata: *Journal of Structural Geology*, v. 26, no. 8, p. 1425–1432, <https://doi.org/10.1016/j.jsg.2004.01.002>.

Cather, S.M., Connell, S.D., Chamberlain, R.M., McIntosh, W.C., Jones, G.E., Potochnik, A.R., Lucas, S.G., and Johnson, P.S., 2008, The Chuska erg: Paleogeomorphic and paleoclimatic implications of an Oligocene sand sea on the Colorado Plateau: *Geological Society of America Bulletin*, v. 120, no. 1–2, p. 13–33, <https://doi.org/10.1130/B26081.1>.

Cawood, P.A., Nemchin, A.A., Freeman, M., and Sircombe, K., 2003, Linking source and sedimentary basin: Detrital zircon record of sediment flux along a modern river system and implications for provenance studies: *Earth*

and Planetary Science Letters, v. 210, no. 1–2, p. 259–268, [https://doi.org/10.1016/S0012-821X\(03\)00122-5](https://doi.org/10.1016/S0012-821X(03)00122-5).

Chapin, C.E., 2008, Interplay of oceanographic and paleoclimate events with tectonism during middle to late Miocene sedimentation across the southwestern USA: *Geosphere*, v. 4, no. 6, p. 976–991, <https://doi.org/10.1130/GES00171.1>.

Clift, P.D., 2010, Enhanced global continental erosion and exhumation driven by Oligo-Miocene climate change: *Geophysical Research Letters*, v. 37, no. 9, L09402, <https://doi.org/10.1029/2010GL043067>.

Davis, S.J., Mulch, A., Carroll, A.R., Horton, T.W., and Chamberlain, C.P., 2009, Paleogene landscape evolution of the central North American Cordillera: Developing topography and hydrology in the Laramide foreland: *Geological Society of America Bulletin*, v. 121, no. 1–2, p. 100–116, <https://doi.org/10.1130/B26308.1>.

Demercian, S., Szatmari, P., and Cobbold, P., 1993, Style and pattern of salt diapirs due to thin-skinned gravitational gliding, Campos and Santos basins, offshore Brazil: *Tectonophysics*, v. 228, no. 3–4, p. 393–433, [https://doi.org/10.1016/0040-1951\(93\)90351-J](https://doi.org/10.1016/0040-1951(93)90351-J).

Diegel, F.A., Karlo, J., Schuster, D., Shoup, R., and Tauvers, P., 1995, Cenozoic structural evolution and tectono-stratigraphic framework of the northern Gulf Coast continental margin, in Jackson, M.P.A., Roberts, D.G., and Snelson, S., eds., *Salt Tectonics: A Global Perspective*: American Association of Petroleum Geologists Memoir 65, p. 109–151.

Dokka, R.K., Sella, G.F., and Dixon, T.H., 2006, Tectonic control of subsidence and southward displacement of southeast Louisiana with respect to stable North America: *Geophysical Research Letters*, v. 33, no. 23, L23308, <https://doi.org/10.1029/2006GL027250>.

Doust, H., 1990, Petroleum geology of the Niger Delta, in Brooks, J., ed., *Classic Petroleum Provinces: Geological Society [London] Special Publication 50*, p. 365–365, <https://doi.org/10.1144/GSL.SP.1990.050.01.21>.

Eaton, G.P., 2008, Epeirogeny in the Southern Rocky Mountains region: Evidence and origin: *Geosphere*, v. 4, no. 5, p. 764–784, <https://doi.org/10.1130/GES00149.1>.

Enzel, Y., Amit, R., Harrison, J.B.J., and Porat, N., 1994, Morphologic dating of fault scarps and terrace risers in the southern Arava, Israel: Comparison to other age-dating techniques and implications for paleoseismicity: *Israel Journal of Earth Sciences*, v. 43, no. 2, p. 91–103.

Fedo, C.M., Sircombe, K.N., and Rainbird, R.H., 2003, Detrital zircon analysis of the sedimentary record: Reviews in Mineralogy and Geochemistry, v. 53, no. 1, p. 277–303, <https://doi.org/10.2113/0530277>.

Fernandes, V.M., Roberts, G.G., White, N., and Whitaker, A.C., 2019, Continental-scale landscape evolution: A history of North American topography: *Journal of Geophysical Research–Earth Surface*, v. 124, no. 11, p. 2689–2722, <https://doi.org/10.1029/2018JF004979>.

Fisk, H.N., 1944, Geological Investigation of the Alluvial Valley of the Lower Mississippi River: Vicksburg, Mississippi, War Department, Corps of Engineers, 78 p.

Fitton, J.G., James, D., and Leeman, W.P., 1991, Basic magmatism associated with late Cenozoic extension in the western United States: Compositional variations in space and time: *Journal of Geophysical Research–Solid Earth*, v. 96, no. B8, p. 13693–13711, <https://doi.org/10.1029/91JB00372>.

Gallen, S.F., Wegmann, K.W., and Bohnenstiehl, D., 2013, Miocene rejuvenation of topographic relief in the southern Appalachians: *GSA Today*, v. 23, no. 2, p. 4–10, <https://doi.org/10.1130/GSATG163A.1>.

Galloway, W.E., 1989, Genetic stratigraphic sequences in basin analysis I: Architecture and genesis of flooding-surface bounded depositional units: *American Association of Petroleum Geologists Bulletin*, v. 73, no. 2, p. 125–142.

Galloway, W.E., 2008, Depositional evolution of the Gulf of Mexico sedimentary basin, in Hsu, J.J., ed., *Sedimentary Basins of the World, Volume 5*: Amsterdam, Netherlands, Elsevier, p. 505–549.

Galloway, W.E., Ganey-Curry, P.E., Li, X., and Buffler, R.T., 2000, Cenozoic depositional history of the Gulf of Mexico basin: *American Association of Petroleum Geologists Bulletin*, v. 84, no. 11, p. 1743–1774.

Galloway, W.E., Blum, M., Marriott, S., and Leclair, S., 2005, Gulf of Mexico basin depositional record of Cenozoic North American drainage basin evolution, in Blum, M.D., Marriott, S.B., and Leclair, S.F., eds., *Fluvial Sedimentology VII: International Association of Sedimentologists Special Publication 35*, p. 409–423.

Galloway, W.E., Whiteaker, T.L., and Ganey-Curry, P., 2011, History of Cenozoic North American drainage basin evolution, sediment yield, and accumulation in the Gulf of Mexico basin: *Geosphere*, v. 7, no. 4, p. 938–973, <https://doi.org/10.1130/GES00647.1>.

Gehrels, G., 2011, Detrital zircon U-Pb geochronology: Current methods and new opportunities, in Busby, C., and Azor, A., eds., *Tectonics of Sedimentary Basins: Recent Advances*: New York, John Wiley and Sons, p. 45–62.

Gradstein, F.M., Ogg, J.G., Schmitz, M., and Ogg, G., 2012, *The Geologic Time Scale 2012*: Amsterdam, Netherlands, Elsevier, 1176 p.

Hackley, P.C., 2012, Geologic Assessment of Undiscovered Conventional Oil and Gas Resources—Middle Eocene Claiborne Group, United States Part of the Gulf of Mexico Basin: U.S. Geological Survey Open-File Report 2012–1144, 87 p., <http://pubs.usgs.gov/of/2012/1144/>.

Hanor, J.S., 1982, Reactivation of fault movement, Tepeate fault zone, south central Louisiana: *Gulf Coast Association of Geological Societies Transactions*, v. 32, p. 237–245.

Haq, B.U., Hardenbol, J., and Vail, P.R., 1987, Chronology of fluctuating sea levels since the Triassic: *Science*, v. 235, no. 4793, p. 1156–1167, <https://doi.org/10.1126/science.235.4793.1156>.

Haughton, P., Todd, S., and Morton, A., 1991, Sedimentary provenance studies, in Morton, A.C., Todd, S.P., and Haughton, P.D.W., eds., *Developments in Sedimentary Provenance Studies: Geological Society [London] Special Publication 57*, p. 1–11, <https://doi.org/10.1144/GSL.SP.1991.057.01.01>.

Heinrich, P., 2000, The De Quincy fault-line scarp: Beaugard and Calcasieu Parishes, Louisiana: *Basin Research Institute Bulletin*, v. 9, p. 38–50.

Heinrich, P., 2008, Loess Map of Louisiana: Baton Rouge, Louisiana, Louisiana Geological Survey Public Information Series 12, 7 p.

Hudec, M.R., and Jackson, M.P., 2007, Terra infirma: Understanding salt tectonics: *Earth-Science Reviews*, v. 82, no. 1–2, p. 1–28, <https://doi.org/10.1016/j.earscirev.2007.01.001>.

Ivins, E.R., Dokka, R.K., and Blom, R.G., 2007, Post-glacial sediment load and subsidence in coastal Louisiana: *Geophysical Research Letters*, v. 34, no. 16, L16303, <https://doi.org/10.1029/2007GL030003>.

Klöcking, M., White, N., MacLennan, J., McKenzie, D., and Fitton, J., 2018, Quantitative relationships between basalt geochemistry, shear wave velocity, and asthenospheric temperature beneath western North America: *Geochemistry Geophysics Geosystems*, v. 19, no. 9, p. 3376–3404, <https://doi.org/10.1029/2018GC007559>.

Klotsko, S., Driscoll, N., Kent, G., and Brothers, D., 2015, Continental shelf morphology and stratigraphy offshore San Onofre, California: The interplay between rates of eustatic change and sediment supply: *Marine Geology*, v. 369, p. 116–126, <https://doi.org/10.1016/j.margeo.2015.08.003>.

Lavier, L.L., Steckler, M.S., and Brigaud, F., 2001, Climatic and tectonic control on the Cenozoic evolution of the West African margin: *Marine Geology*, v. 178, no. 1–4, p. 63–80, [https://doi.org/10.1016/S0025-3227\(01\)00175-X](https://doi.org/10.1016/S0025-3227(01)00175-X).

Liu, L., 2014, Rejuvenation of Appalachian topography caused by subsidence-induced differential erosion: *Nature Geoscience*, v. 7, no. 7, p. 518–523, <https://doi.org/10.1038/ngeo2187>.

Liu, L., 2015, The ups and downs of North America: Evaluating the role of mantle dynamic topography since the Mesozoic: *Reviews of Geophysics*, v. 53, no. 3, p. 1022–1049, <https://doi.org/10.1002/2015RG000489>.

Lopez, J.A., 1990, Structural styles of growth faults in the U.S. Gulf Coast Basin, in Brooks, J., ed., *Classic Petroleum Provinces: Geological Society [London] Special Publication 50*, p. 203–219, <https://doi.org/10.1144/GSL.SP.1990.050.01.10>.

- Mansfield, C., and Cartwright, J., 1996, High resolution fault displacement mapping from three-dimensional seismic data: Evidence for dip linkage during fault growth: *Journal of Structural Geology*, v. 18, no. 2, p. 249–263, [https://doi.org/10.1016/S0191-8141\(96\)80048-4](https://doi.org/10.1016/S0191-8141(96)80048-4).
- McBride, B.C., 1998, The evolution of allochthonous salt along a megaregional profile across the northern Gulf of Mexico Basin: *American Association of Petroleum Geologists Bulletin*, v. 82, no. 5, p. 1037–1054.
- McFarlan, E., Jr., and LeRoy, D., 1988, Subsurface geology of the late Tertiary and Quaternary deposits, coastal Louisiana and the adjacent continental shelf: *Gulf Coast Association of Geological Societies Transactions*, v. 38, p. 421–433.
- McMillan, M.E., Angevine, C.L., and Heller, P.L., 2002, Postdepositional tilt of the Miocene–Pliocene Ogallala Group on the western Great Plains: Evidence of late Cenozoic uplift of the Rocky Mountains: *Geology*, v. 30, no. 1, p. 63–66, [https://doi.org/10.1130/0091-7613\(2002\)030<0063:PTOTMP>2.0.CO;2](https://doi.org/10.1130/0091-7613(2002)030<0063:PTOTMP>2.0.CO;2).
- McMillan, M.E., Heller, P.L., and Wing, S.L., 2006, History and causes of post-Laramide relief in the Rocky Mountain orogenic plateau: *Geological Society of America Bulletin*, v. 118, no. 3–4, p. 393–405, <https://doi.org/10.1130/B25712.1>.
- Miller, K.G., Kominz, M.A., Browning, J.V., Wright, J.D., Mountain, G.S., Katz, M.E., Sugarman, P.J., Cramer, B.S., Christie-Blick, N., and Pekar, S.F., 2005, The Phanerozoic record of global sea-level change: *Science*, v. 310, no. 5752, p. 1293–1298, <https://doi.org/10.1126/science.1116412>.
- Miller, K.G., Mountain, G.S., Wright, J.D., and Browning, J.V., 2011, A 180-million-year record of sea level and ice volume variations from continental margin and deep-sea isotopic records: *Oceanography* (Washington, D.C.), v. 24, no. 2, p. 40–53, <https://doi.org/10.5670/oceanog.2011.26>.
- Miller, K.G., Browning, J.V., Schmelz, W.J., Kopp, R.E., Mountain, G.S., and Wright, J.D., 2020, Cenozoic sea-level and cryospheric evolution from deep-sea geochemical and continental margin records: *Science Advances*, v. 6, no. 20, p. eaaz1346, <https://doi.org/10.1126/sciadv.aaz1346>.
- Miller, S.R., Sak, P.B., Kirby, E., and Bierman, P.R., 2013, Neogene rejuvenation of central Appalachian topography: Evidence for differential rock uplift from stream profiles and erosion rates: *Earth and Planetary Science Letters*, v. 369, p. 1–12, <https://doi.org/10.1016/j.epsl.2013.04.007>.
- Molnar, P., 2001, Climate change, flooding in arid environments, and erosion rates: *Geology*, v. 29, no. 12, p. 1071–1074, [https://doi.org/10.1130/0091-7613\(2001\)029<1071:CCFIAE>2.0.CO;2](https://doi.org/10.1130/0091-7613(2001)029<1071:CCFIAE>2.0.CO;2).
- Mountain, G.S., Burger, R.L., Delius, H., Fulthorpe, C.S., Austin, J.A., Goldberg, D.S., Steckler, M.S., McHugh, C.M., Miller, K.G., and Monteverde, D.H., 2007, The long-term stratigraphic record on continental margins, in Jarvis, I., Nittrouer, C.A., Austin, J.A., Field, M.E., Kravitz, J.H., Syvitski, J.P.M., and Wiberg, P.L., eds., *Continental Margin Sedimentation: From Sediment Transport to Sequence Stratigraphy*: International Association of Sedimentologists Special Publication 37, p. 381–458, <https://doi.org/10.1002/9781444304398.ch8>.
- Nunn, J.A., 1985, State of stress in the northern Gulf Coast: *Geology*, v. 13, no. 6, p. 429–432, [https://doi.org/10.1130/0091-7613\(1985\)13<429:SOSITN>2.0.CO;2](https://doi.org/10.1130/0091-7613(1985)13<429:SOSITN>2.0.CO;2).
- Ojeda, H., 1982, Structural framework, stratigraphy, and evolution of Brazilian marginal basins: *American Association of Petroleum Geologists Bulletin*, v. 66, no. 6, p. 732–749.
- Omale, A.P., and Lorenzo, J.M., 2015, Using fault kinematics to evaluate the relationship between Cenozoic fault activity, sedimentation rates, and salt movement in the Gulf of Mexico: A comparison between southwestern and southeastern Louisiana: *Gulf Coast Association of Geological Societies Journal*, v. 4, p. 132–146.
- Pazzaglia, F.J., and Brandon, M.T., 1996, Macrogeomorphic evolution of the post-Triassic Appalachian mountains determined by deconvolution of the offshore basin sedimentary record: *Basin Research*, v. 8, no. 3, p. 255–278, <https://doi.org/10.1046/j.1365-2117.1996.00274.x>.
- Peel, F., Travis, C., and Hossack, J., 1995, Genetic structural provinces and salt tectonics of the Cenozoic offshore U.S. Gulf of Mexico: A preliminary analysis, in Jackson, M.P.A., Roberts, D.G., and Snelson, S., eds., *Salt Tectonics: A Global Perspective*: American Association of Petroleum Geologists Memoir 65, p. 153–175.
- Posamentier, H., 1988, Eustatic controls on clastic deposition II—Conceptual framework, in Wilgus, C.K., et al., eds., *Sea-Level Changes: An Integrated Approach*: Society of Economic Paleontologists and Mineralogists (SEPM) Special Publication 42, p. 125–154, <https://doi.org/10.2110/pec.88.01.0125>.
- Posamentier, H., Jervey, M., and Vail, P., 1988, Eustatic controls on clastic deposition I—conceptual framework, in Wilgus, C.K., et al., eds., *Sea-Level Changes: An Integrated Approach*: Society of Economic Paleontologists and Mineralogists (SEPM) Special Publication 42, p. 109–124, <https://doi.org/10.2110/pec.88.01.0109>.
- Rainwater, E., 1964, Regional stratigraphy of the Gulf Coast Miocene: *Gulf Coast Association of Geological Societies Transactions*, v. 14, p. 81–124.
- Rao, G., Cheng, Y., Lin, A., and Yan, B., 2017, Relationship between landslides and active normal faulting in the epicentral area of the AD 1556 M_w 8.5 Huaxian earthquake, SE Weihe graben (central China): *Journal of Earth Science*, v. 28, no. 3, p. 545–554, <https://doi.org/10.1007/s12583-017-0900-z>.
- Rasmussen, E., 2004, The interplay between true eustatic sea-level changes, tectonics, and climatic changes: What is the dominating factor in sequence formation of the Upper Oligocene–Miocene succession in the eastern North Sea Basin, Denmark?: *Global and Planetary Change*, v. 41, no. 1, p. 15–30, <https://doi.org/10.1016/j.gloplacha.2003.08.004>.
- Retallack, G.J., 2007, Cenozoic paleoclimate on land in North America: *The Journal of Geology*, v. 115, no. 3, p. 271–294, <https://doi.org/10.1086/512753>.
- Rowan, M.G., 1995, Structural styles and evolution of allochthonous salt, central Louisiana outer shelf and upper slope, in Jackson, M.P.A., Roberts, D.G., and Snelson, S., eds., *Salt Tectonics: A Global Perspective*: American Association of Petroleum Geologists Memoir 65, p. 199–228, <https://doi.org/10.1306/M65604C9>.
- Rowan, M.G., 2019, Conundrums in loading-driven salt movement: *Journal of Structural Geology*, v. 125, p. 256–261, <https://doi.org/10.1016/j.jsg.2018.04.010>.
- Rowan, M.G., Jackson, M.P., and Trudgill, B.D., 1999, Salt-related fault families and fault welds in the northern Gulf of Mexico: *American Association of Petroleum Geologists Bulletin*, v. 83, no. 9, p. 1454–1484.
- Rowan, M.G., Peel, F.J., Vendeville, B.C., and Gaullier, V., 2012, Salt tectonics at passive margins: Geology versus models—Discussion: *Marine and Petroleum Geology*, v. 37, no. 1, p. 184–194, <https://doi.org/10.1016/j.marpetgeo.2012.04.007>.
- Roy, M., Jordan, T.H., and Pederson, J., 2009, Colorado Plateau magmatism and uplift by warming of heterogeneous lithosphere: *Nature*, v. 459, no. 7249, p. 978–982, <https://doi.org/10.1038/nature08052>.
- Salvador, A., 1987, Late Triassic–Jurassic paleogeography and origin of Gulf of Mexico basin: *American Association of Petroleum Geologists Bulletin*, v. 71, no. 4, p. 419–451.
- Sandwell, D.T., and Smith, W.H., 2005, Retracking ERS-1 altimeter waveforms for optimal gravity field recovery: *Geophysical Journal International*, v. 163, no. 1, p. 79–89, <https://doi.org/10.1111/j.1365-246X.2005.02724.x>.
- Saucier, R.T., 1994, Geomorphology and Quaternary Geologic History of the Lower Mississippi Valley: Vicksburg, Mississippi, U.S. Army Corps of Engineer Waterways Experiment Station Geotechnical Laboratory, 2 volumes.
- Sawyer, D.S., Buffler, R.T., and Pilger, R.H., Jr., 1991, The crust under the Gulf of Mexico basin, in Salvador, A., ed., *The Gulf of Mexico Basin*: Boulder, Colorado, Geological Society of America, *The Geology of North America*, v. J, p. 53–72, <https://doi.org/10.1130/DNAG-GNA-J.53>.
- Schuster, D., 1996, Deformation of allochthonous salt and evolution of related salt-structural systems, eastern Louisiana Gulf Coast, in Jackson, M.P.A., Roberts, D.G., and Snelson, S., eds., *Salt Tectonics: A Global Perspective*: American Association of Petroleum Geologists Memoir 65, p. 177–198.
- Sewall, J.O., and Sloan, L.C., 2006, Come a little bit closer: A high-resolution climate study of the early Paleogene Laramide foreland: *Geology*, v. 34, no. 2, p. 81–84, <https://doi.org/10.1130/G22177.1>.
- Shen, Z., Dawers, N.H., Törnquist, T.E., Gasparini, N.M., Hijma, M.P., and Mauz, B., 2017, Mechanisms of late Quaternary fault throw-rate variability along the north central Gulf of Mexico coast: Implications for coastal subsidence: *Basin Research*, v. 29, no. 5, p. 557–570, <https://doi.org/10.1111/bre.12184>.
- Tearpock, D.J., and Bischke, R.E., 2003, *Applied Subsurface Geological Mapping: With Structural Methods*: Upper Saddle River, New Jersey, Prentice Hall, 822 p.
- Thompson, R.S., 1991, Pliocene environments and climates in the western United States: *Quaternary Science Reviews*, v. 10, no. 2–3, p. 115–132.
- Thorsen, C., 1963, Age of growth faulting in southeast Louisiana: *Gulf Coast Association of Geological Societies Transactions*, v. 13, p. 103–110.
- Vail, P., Mitchum, R., Jr., and Thompson, S., III, 1977, Seismic stratigraphy and global changes of sea level: Part 4. Global cycles of relative changes of sea level: Section 2. Application of seismic reflection configuration to stratigraphic interpretation, in Payton, C.E., ed., *Seismic Stratigraphy—Applications to Hydrocarbon Exploration*: American Association of Petroleum Geologists Memoir 26, p. 83–97.
- Van der Zwan, C., 2002, The impact of Milankovitch-scale climatic forcing on sediment supply: *Sedimentary Geology*, v. 147, no. 3–4, p. 271–294, [https://doi.org/10.1016/S0037-0738\(01\)00130-0](https://doi.org/10.1016/S0037-0738(01)00130-0).
- Van Wagoner, J., Posamentier, H., Mitchum, R., Vail, P., Sarg, J., Loutit, T., and Hardenbol, J., 1988, An overview of the fundamentals of sequence stratigraphy and key definitions, in Wilgus, C.K., et al., eds., *Sea-Level Changes: An Integrated Approach*: Society of Economic Paleontologists and Mineralogists (SEPM) Special Publication 42, p. 39–45, <https://doi.org/10.2110/pec.88.01.0039>.
- Vendeville, B., and Jackson, M., 1992a, The fall of diapirs during thin-skinned extension: *Marine and Petroleum Geology*, v. 9, no. 4, p. 354–371, [https://doi.org/10.1016/0264-8172\(92\)90048-J](https://doi.org/10.1016/0264-8172(92)90048-J).
- Vendeville, B.C., and Jackson, M.P., 1992b, The rise of diapirs during thin-skinned extension: *Marine and Petroleum Geology*, v. 9, no. 4, p. 331–354, [https://doi.org/10.1016/0264-8172\(92\)90047-I](https://doi.org/10.1016/0264-8172(92)90047-I).
- Walgenwitz, F., Richert, J., and Charpentier, P., 1992, Southwest African plate margin: Thermal history and geodynamical implications, in Poag, C.W., and de Graciansky, P.C., eds., *Geologic Evolution of Atlantic Continental Rises*: New York, Van Nostrand Reinhold, p. 20–45, https://doi.org/10.1007/978-1-4684-6500-6_2.
- Wallace, R.E., 1977, Profiles and ages of young fault scarps, north-central Nevada: *Geological Society of America Bulletin*, v. 88, no. 9, p. 1267–1281, [https://doi.org/10.1130/0016-7606\(1977\)88<1267:PAAOYF>2.0.CO;2](https://doi.org/10.1130/0016-7606(1977)88<1267:PAAOYF>2.0.CO;2).
- Weissert, H., Joachimski, M., and Sarntheim, M., 2008, Chemostratigraphy: Newsletters on Stratigraphy, v. 42, no. 3, p. 145–179, <https://doi.org/10.1127/0078-0421/2008/0042-0145>.
- Whiteman, A., 1982, *Nigeria: Its Petroleum Geology: Resources and Potential*, Volume 2: Berlin, Springer, 394 p.
- Wilf, P., 2000, Late Paleocene–early Eocene climate changes in southwestern Wyoming: Paleobotanical analysis: *Geological Society of America Bulletin*, v. 112, no. 2, p. 292–307, [https://doi.org/10.1130/0016-7606\(2000\)112<292:LPECCI>2.0.CO;2](https://doi.org/10.1130/0016-7606(2000)112<292:LPECCI>2.0.CO;2).
- Winker, C.D., 1982, Cenozoic shelf margins: Northwestern Gulf of Mexico basin: *Gulf Coast Association of Geological Societies Transactions*, v. 32, p. 427–448.
- Winker, C.D., and Buffler, R.T., 1988, Paleogeographic evolution of early deep-water Gulf of Mexico and margins, Jurassic to Middle Cretaceous (Comanchean): *American Association of Petroleum Geologists Bulletin*, v. 72, no. 3, p. 318–346.
- Woodbury, H., Murray, I., Jr., Pickford, P., and Akers, W., 1973, Pliocene and Pleistocene depocenters, outer continental shelf, Louisiana and Texas: *American As-*

- sociation of Petroleum Geologists Bulletin, v. 57, no. 12, p. 2438–2439.
- Worrall, D., and Snelson, S., 1989, Evolution of the northern Gulf of Mexico, *in* Bally, A.W., and Palmer, A.R., eds., *The Geology of North America—An Overview: Geology of North America*, v. A, p. 97–138, <https://doi.org/10.1130/DNAG-GNA-A.97>.
- Wu, S., Bally, A.W., and Cramez, C., 1990, Allochthonous salt, structure and stratigraphy of the north-eastern Gulf of Mexico. Part II: Structure: *Marine and Petroleum Geology*, v. 7, no. 4, p. 334–370, [https://doi.org/10.1016/0264-8172\(90\)90014-8](https://doi.org/10.1016/0264-8172(90)90014-8).
- Xu, J., Snedden, J.W., Stockli, D.F., Fulthorpe, C.S., and Galoway, W.E., 2017, Early Miocene continental-scale sediment supply to the Gulf of Mexico basin based on detrital zircon analysis: *Geological Society of America Bulletin*, v. 129, no. 1–2, p. 3–22, <https://doi.org/10.1130/B31465.1>.
- Zachos, J., Pagani, M., Sloan, L., Thomas, E., and Billups, K., 2001, Trends, rhythms, and aberrations in global climate 65 Ma to present: *Science*, v. 292, no. 5517, p. 686–693, <https://doi.org/10.1126/science.1059412>.

SCIENCE EDITOR: BRAD S. SINGER
ASSOCIATE EDITOR: ENRICO TAVARNELLI

MANUSCRIPT RECEIVED 9 JANUARY 2020
REVISED MANUSCRIPT RECEIVED 31 AUGUST 2020
MANUSCRIPT ACCEPTED 25 NOVEMBER 2020

Printed in the USA